21-7-2024

Developing customized CSI data collection hardware for human presence sensing in indoor and outdoor environments.

Abstract:

In this bachelor thesis, the possibilities and challenges of CSI sensing will be explored. The question which hardware is required for effective and energy-efficient CSI analysis will be answered, as well as research questions about the effectiveness of a particular microcontroller series for these types of applications. Several real-world tests and experiments will be conducted in order to determine which parts are the most suitable for the given design requirements. A very detailed insight will be given into the determination of the design requirements of the custom hardware solution, as well as the design process itself using these set requirements. The entire project is open-source, and all the design and development files of the custom hardware solution will be uploaded to the internet.

Hugo van 't Riet
CREATIVE TECHNOLOGY BACHELOR THESIS
SUPERVISOR: JEROEN KLEIN BRINKE
CRITICAL OBSERVER: ANDREAS KAMILARIS

Acknowledgement

In this acknowledgement, I would like to express my gratitude towards several people who supported me in writing this bachelor thesis. First, I would like to thank dr. ir. Jeroen Klein Brinke for his proposal to work together on this project. I was approached by him with the idea to combine our projects into a collaboration project. For the CSI-related research of Jeroen he wanted to use customized hardware to make the research and development process easier. Common off-the-shelve development boards did not suit all the needs of the research, which made customized research hardware a logical next step. When I was looking for a suitable graduation project, I did not find many hardware related proposal projects provided by the study. Since I wanted to make my graduation project about something I truly like and am passionate about, I was looking for a project which involved hardware design including PCB development. Because we would both benefit from this collaboration, we decided to work together on this project. Since Jeroen was not only my client for this project but also my supervisor, we were able to tightly integrate both of our interests into this project, which made the collaboration pleasant.

Because Jeroen is my client as well as supervisor, a potential conflict of interests can occur easily. This is why an additional critical observer is of great importance of this project to make sure that the report is entirely up to the required academic standards. I would like dr. Andreas Kamilaris for being the critical observer for this project. Without the verification provided by him, this report would not hold any academic credibility.

Last but certainly not least, I would like to thank all the participants who actively supported this work by helping me with the experiments. The results provided by the experiments gave useful insights which were referred to several times throughout this report. The help with the experiments was essential for being able to draw conclusions, without the help of the participants it was not possible to finish this report.

Contents

Introduction

There are several technologies available for human presence detection and object recognition, like radar waves using very high frequencies between 24GHz and 300GHz, and light/ultrasound sensors responding to reflections. Radar and optical/ultrasound sensors are emitting signals themselves and rely on reflection of this signal in order to output a result.

These types of sensors have been applied in large numbers over the years for all kinds of applications, mostly to enable and disable devices depending on whether there are people nearby. An example of such applications could be (office) lighting or audio systems that enable and disable themselves on demand.

Although these systems work great for simple applications, like switching certain devices on and off, it can still only provide a binary output. Eighter there are people nearby, or not. This characteristic does not allow these systems to be applied for more complicated tasks. An example of a more complicated task is to increase and decrease the brightness of outdoor streetlights based on the position of someone on a road. This cannot be achieved with a single binary-type sensor since the system then cannot determine which specific light to turn up or down in brightness.

Another problem with the mentioned active sensing methods is that they are constantly required to send out signals in order to make use of the reflective nature of the sent out signals. Because signals need to be sent independently of human presence or system activity, this is essentially wasted energy when there is no one present or if there are no objects placed in the detection area. A possible alternative would be to use signals that are already emitted by other devices in order to take measurements, instead of active sensing by emitting signals from the sensor and thereby relying on reflections of the sent out signal.

Other than that, some materials or conditions are also known to absorb or manipulate particular wavelengths, which would make sensing more difficult. IR sensors for example are often used for indoors applications, but they rely on the reflection of this IR light. When placed outside, there is a lot of background IR light available, making sensing with this technique a difficult task. The same goes for ultrasonic sensors. These sensors emit sounds that are inaudible for the human hearing range. Sounds can easily be absorbed by carpeting on floors or foam sealing panels, which could invalidate the sensing results.

Since all mentioned human presence detection techniques mentioned so far have their own benefits and drawbacks, none of them are the perfect solution for every problem. A possible alternative to the mentioned human presence detection techniques would be a passive sensing method that measure changes in the environment without transmitting any signals from the sensor. Changes in a given environment caused by human presence could then be sensed and processed.

Everywhere around us in the modern world are already several kinds of radio waves. There are billions of devices with some type of wireless radio on-board. IoT devices are an important contributor to this. Currently, there are around fifteen billion [1] of such IoT devices, and this number is still increasing. The most applied communication technology for IoT devices is Wi-Fi. With billions of sources sending out signals on the 2.4GHz band, the potential for alternative functions of these signals become significant.

Wi-Fi has a hidden data collection feature that is not relevant to the end user but could potentially be relevant to device manufacturers and researchers. This feature is called channel state information (CSI for short). CSI is used by Wi-Fi devices like routers to compensate for reflections and disruptions of the Wi-Fi signal. Smart algorithms in routers are designed to calculate how the signal propagates towards the target device, and to compensate for it during transmission.

Since the CSI contains information on how signals reflect within a given space, it could also be used for estimating the position of people or objects within a given space.

This project will focus on designing a non-invasive, easy to implement, and power-efficient sensor module using CSI technology for human presence detection and object recognition purposes. The sensor module will be designed for the purpose of replacing conventional human presence sensing techniques, for applications where these techniques will not suffice. The module will be able to be applied in indoor and outdoor environments.

Autonomous operation will be an important consideration for the final design. Since the sensor should be applicable for both indoor and outdoor applications, the design will include a circuit the sensor needs to collect power from its environment and to store this collected power to be able to use it later. For indoor applications autonomous operation is less important. The sensor modules will be equipped in such a way that they are able to operate with a power source nearby as well instead of relying on energy storage and energy harvesting systems.

To achieve sustained autonomous operation, energy efficiency of the sensor module is an important aspect. When power is not used in an effective and thoughtful way, it becomes significantly more difficult to keep the module working in an autonomous way for a long time. Hardware and software choices must be made in such a way that energy usage is limited, making autonomous operation possible for an extended time.

For improved accuracy and precision, the module will use multiple antennas. The usage of multiple antennas allows the module to not only estimate if someone is standing in a given space, but also estimate where someone is standing with a high accuracy and precision level. Using multiple antennas placed in different places on the device allows for more data processing possibilities.

To increase the simplicity of implementation even further, the sensor module will be designed to be as compact as possible without sacrificing on functionality. A smaller size makes integration with existing products and setups easier. Other physical aspects which are required for the module are to fit a weatherproof casing for outdoor usage. In the design process, special care and attention will be taken to ensure that the module will not only comply to the electrical/hardware requirements, but also the physical requirements.

Once the design process has been completed, several experiments will be conducted to simulate real-world scenarios. These experiments will be useful for validating the design and determining if it could be applied in practice. If the experiments return unexpected results, it is an indication that the proposed design is not completed yet, and revision is required in order to achieve the intended outcome.

Possible future experiments and developments are also discussed after the results are collected. The questions of possible future improvements to the design and other research possibilities will be answered in order to find new potential benefits, downsides, and applications for CSI-based technology in the field of human presence detection.

Background research

Research questions

Given the subjects of interest of this research, the following research question and sub-questions were selected:

- **Research question:** Is CSI-based position estimation and object recognition a feasible replacement for other technologies like radar?
    - **Sub question 1:** For which type of applications are CSI-based systems usable?
    - **Sub question 2:** What level of accuracy can be achieved with CSI-based systems?
    - **Sub question 3:** What are desired environmental conditions for CSI-technology?
    - **Sub question 4:** Which type of MCUs/sensors are typically used in other research involving CSI-technology?

Possibilities of CSI-systems

Because CSI technology is so versatile in its application possibilities, it has been applied in numerous unique applications. Some systems using CSI are fairly simple in nature like simply telling if there are humans nearby (R. Zhou et al. [2] and S. Palipana et al. [9]) or identifying pre-trained objects (T. Murakami et al. [6] and M. Peng et al. [7]), but other systems using CSI are used for more advanced applications like estimating the walking/running speed of humans (K. Qian et al. [5]) and recognizing dangerous items and estimating the size of fluid containers in air travel luggage (C. Wang et al. [8]). This makes CSI technology very versatile, and applicable for simple tasks, as well as more complex tasks.

When combining CSI with camera input, and an AI model is trained with both the camera input and CSI data, it is even possible to train the system to estimate the poses of people with just CSI data without the camera input (F. Wang et al. [13]). This essentially means that it would be possible to build a system that can see in the dark and through walls. This project in particular will not contain any camera input combined with AI algorithms, but the fact that it is possible to determine the position and pose of someone in a different room without the use of cameras or the requirement of light is a great example of the things CSI-based technology can achieve.

Accuracy of CSI-based systems

For applications like crowd size estimation and object recognition, CSI-based systems can be a suitable choice. O. Oshiga et al. [3] indicates that for the purpose of crowd size estimation within a given space accuracies as high as 100% can be reached, depending on the used classifier algorithm and the input training data. According to C. Wang et al. [8], it is even possible to use this technique as an airport security system. It is possible to determine the type of material objects in a suitcase are made from, as well as liquid volume estimation. It was possible to estimate the volume of a liquid container using a linear regression model with more than 80% of the estimation errors being off by less than 35ml. When using the neural network, the accuracy was increased to a standard error of just 16ml among all the samples taken. With these accuracy numbers in mind, it is safe to assume that CSI-based systems can be applied in various accuracy sensitive applications with good results. As long as there is enough training data and the chosen analysis algorithm suits the application, low tolerance accuracy results can be expected with CSI-technology.

CSI-based technology is accurate enough for static purposes like human presence detection and object recognition. It is even possible to detect dynamic events, like human movement with CSI-based sensing. T. Hang et al. [4] indicated that the accuracy for motion detection is lower for true positive events (a person actually moving) than for true negative events (a person actually standing still). True positive accuracy scores an accuracy score of 81.5% on average, while true negative scores 92.9% on average, making the technology more trustworthy in detecting stationary people compared

to people in motion. K. Qian et al [5] was able to achieve a higher accuracy number of almost equal to 100% accuracy for true negative cases in all four tested areas, and an accuracy of more than 93% for true positive cases. Both experiments used similar hardware, namely the intel 5300 NIC. Therefore, this part of the test setup is in both cases identical. The way the data is filtered and interpreted is different in both experiments, which causes the different results. Therefore, the algorithms used to filter out noise and the algorithms converting the raw data into output data are of significant influence.

Conditions for successful applications of CSI-systems

CSI-systems can be applied in various different environments and settings. K. Qian et al. [5] suggests that the size of the area used with CSI is not important, only the distance between the sending and receiving nodes, and if there are any obstacles in between the sender and receiver. This claim is further supported by research conducted by M. Peng et al. [7]. It was found that if the distance between the two nodes increases, the fading and weakening of the signal increases. This makes the signal more vulnerable to noise, which makes calculating the output more complex and less predictable and accurate. Because the link length has a very significant influence on the output accuracy of the system, it is important to keep this variable in mind when designing a CSI-system. The difference in accuracy between 2 and 3 meter can be as high as 5%, dropping from almost 100% accuracy to 95%. Therefore, it is desirable to keep the link length no larger than 2 meter in order to achieve the most accurate results.

The benefit of having already many Wi-Fi devices available to send out CSI packages can also be a disadvantage if not accounted for. O. Oshiga et al. [3] found that due to many devices being already Wi-Fi capable, the 2.4GHz band can become loaded in some cases. Often these devices all transmit on the same Wi-Fi channel, causing more noise on received packages which makes analyzing more difficult. C. M. Mesa-Cantillo et al [11] claims that multiple devices can be beneficial for the accuracy of the measurements, but only one transmitting node and multiple receiving nodes. By applying this method, the 2.4GHz band will not be stressed with too much transmitting data, but more receivers do allow for more detailed analysis because there is more input data. If there are multiple devices transmitting on the same channel in an area, the problem can also be solved by changing the channel on those devices or using a free channel for the CSI setup.

Hardware used for CSI-systems

For research in CSI, the hardware/software combination most often used is the Intel 5300 NIC combined with some type of Linux distribution. Of all the literature analyzed in this report, at least seven sources (R. Zhou et al. [2], O. Oshiga et al[3], T. Hang et al. [4], K. Qian et al. [5], C. Wang et al. [8], S. Palipana et al. [9] and C. Han et al. [10]) confirmed the usage of this combination of hardware and software. This particular combination is suitable for the usage of the 'Linux 802.11n CSI tool', a very popular open-source solution for CSI data analysis [12]. Although the routers and APs used in the studies are a different make and model, they all have the same transmission protocol, namely 802.11n. This is a variant of the 802.11 standard with support for MIMO (multiple input multiple output). MIMO is essential for accurate CSI analysis, since MIMO routers have at least two antennas, making it possible to accurately localize the object or person. The general setup used for CSI-systems can be summarized as the receiver being an Intel 5300 NIC with customized firmware running on a Linux operating system, and a transmitter with multiple antennas with 802.11n support.

CSI-technology has the potential to be very accurate, if set-up properly and if the analyzing algorithm has been trained or modified for the application environment. Filtering away the noise emitted by other devices on the same channel, or preventing noise by switching nearby devices to appropriate channels does also drastically improve accuracy results. The more attention is paid, and time is given to developing the analysis algorithm, the better the final output accuracy results.

Optimal operating conditions for all CSI-based systems investigated can be summarized as no to very little interference on the same channels as the CSI system is running on and keeping the link length between nodes as short as reasonably possible with a clear line of sight between nodes without obstructions. The effect that the size of the room has on the accuracy is very limited to non-existent, only the placement of the nodes within this given space is of significant importance.

Due to limitations set for this project, it is not feasible to apply a full computer running an operating system with a network interface card for CSI-analysis. These systems consume too much power and are too large for a non-invasive and energy-efficient system. Therefore it is required to look at alternative methods than mentioned in most earlier CSI experiments.

Literature matrix

RQ\source	Device-free Presence Detection and Localization with SVM and CSI-Fingerprinting [2]	Human Detection For Crowd Count Estimation Using CSI for WiFi Signals [3]	WiSH: WiFi-Based Real-Time Human Detection [4]	Enabling Contactless Detection of Moving Humans with Dynamic Speeds Using CSI [5]	Wireless LAN-Based CSI Monitoring System for Object Detection [6]	Wi-Tar: Object Detection System Based on CSI Ratio [7]	Towards In-baggage Suspicious Object Detection Using Commodity WiFi [8]	Channel State Information Based Human Presence Detection using Non-linear Techniques [9]	CSI Frequency Domain Fingerprint-Based Passive Indoor Human Detection [10]	A Non Intrusive Human Presence Detection Methodology Based on CSI of Wi-Fi Networks [11]	**Synthesis**
What level of accuracy can be achieved with CSI-based systems?	'Evaluations prove the effectiveness of the algorithm, achieving localization accuracy of 1.22m in the research laboratory and 1.39m in the meeting room, and presence detection precision of more than 97%'	'Results in Table I shows the results of crowd estimation for different number of people in a room using early fusion and late fusion. As the statistics show, late fusion performs better since it exploits six different channels with six different classifiers. Though each classifier is weaker compared to that of early fusion, more channels provide more information for human presence detection.'	'Results demonstrate that WiSH achieves grateful detection performance even with a low sampling rate of 20 Hz on resource-limited devices. Specifically, WiSH yields a detection accuracy of >98%. The average detection delay is 1.5 s, whereas the durations of all detected events overlap with true events by 76.7%, which grows to 92.5% if the sampling rate increases to 90 Hz.'	'Experiment results in different scenarios including the laboratory, classrooms, corridors, and meeting rooms demonstrate that PADS achieves great performance in spite of dynamic human movements (various walking speed). Concretely, PADS accurately alarms human movements by 99% on average with almost no false-negative errors.'	'To further improve the accuracy, channel state information (CSI) was studied by utilizing channel responses, which included received power values per subcarrier on the orthogonal frequency division multiplexing (OFDM) transmission. They also included relative values (power and phase information) between transmitter and receiver antennas via multiple input multiple output (MIMO) transmission'	'The detection accuracy for objects located near the transmitter and receiver is slightly lower than that for objects near the midpoint of the link line, but all can detect different materials with an accuracy of over 98%. When the object is placed at a position of 0.4 m and 1.6 m, it can identify ordinary objects and liquids with an accuracy of over 98.5%. When objects are placed in positions of 0.8 m and 1.2 m, the accuracy of detecting ordinary objects and liquids exceeds 99%.'	'In particular, given the combination of all the 15 objects and the 6 bags in our profile, Figure 12(a) shows that our system can achieve 99% accuracy in classifying dangerous objects from non-dangerous (step1) and 97% accuracy to further differentiate the dangerous objects to be metal and liquid (step2). Figure 12(b) further shows that the overall detection rate for the dangerous material, metal and liquid are 99%, 98% and 95%.'	'Highest detection percentages in general are for the two dynamic scenarios and for positions near the link such as s12, s23,s32, s43, s52 and s53. Lowest detections are generally for positions far away from the link such as s11, s21 and s41. This behaviour can be explained as follows. When a person is closer to the LoS, more paths get affected. The number of paths disturbed by the person far away from the link are less and have weak amplitudes so they do not cause large perturbations in CSI.'	'When 500 packets are used, the static detection rate is 96.67%, a static target detection rate 90.89%, and the dynamic detection rate 100%. When 750 packets are used, the static detection rate is 97.5%, the static target detection rate is 92.58%, and the dynamic detection rate is 100%. Based on the assumption that the detection rates of all three states should be above 90%, the minimum number of packets required for the training set and the online test set is 500.'	'As shown in Section 6, we conclude that the linear SVM classifier was the most suitable in this case and scenario since it has an accuracy rate over 92% in all the scenarios and tests. In addition, we can conclude that, with this parameter setting and the classification learner app, it is possible to determine when a human interference is occurring. One of the limitations of the system is that it is only able to detect one intrusion at a time, and it is not able to distinguish whether the intrusion has been caused by one or several people.'	**Accuracy is defined differently depending on the purpose of the CSI sensing system. Depending on the input training data and filtering algorithm used, very high accuracy numbers can be achieved. Factors like the position of a person/object in the room and the placement of the stations can alter accuracy. The optimal place for sensing is between two nodes with a somewhat similar distance between the object/person and the two nodes. The more samples used for training, the better the accuracy of the final application.**

What are desired environmental conditions for CSI-technology?	The localization results with CSI and SVR in the research laboratory and the meeting room are shown in Fig. 8. In the research laboratory, the accuracy is 1.22 m, and the minimal and the maximal error distances are 0.01 m and 2.91 m, respectively. The error distance is within 1 m with the probability of 51.7%, within 2 m 83.9%, and within 3 m 100%. In the meeting room, the accuracy is 1.39 m, and the minimal and the maximal error distances are 0.28 m and 2.76 m, respectively. The error distance is within 1 m with the probability of 35.0%, within 2 m 91.0%, and within 3 m 100%	'First, due to interference caused by commercial WiFi devices in the same channel, packets received are extremely noisy and not evenly distributed in time.'	'We observe that the ME-TP rate exceeds 98% in both scenarios. The MD-TP rate (duration accuracy) is relatively low compared with the ME-TP rate (event accuracy). It is rational if we take the speed of the moving target, sensitivity variety at different locations, and other factors into consideration, which are comprehensively discussed hereinafter. False alarms can be further minimized if we choose a channel that suffers less radio frequency interference as other devices may operate in the same channel.'	'The three detection systems work well in regular rooms like the classroom, lab, and meeting room, which means that the size of and furniture in the room have little impact on performance. However, the three systems experience the same trend of degradation of performance in the corridor, though to different extent, which means that the shape of the monitor area plays an important role.'	'The bandwidth is 20 MHz and the AP, CSI monitoring station, and CSI measuring station have respectively four, four, and two antennas. In the conventional system, we assumed that in order to communicate with the stations of the cell edge, the transfer scheme between the AP and CSI measuring station is QPSK (Quadrature Phase Shift Keying), 1/2 convolutional rate, and two streams on MIMO transmission. In the proposed system, it is QPSK or 16QAM (Quadrature Amplitude Modulation), 1/2 convolutional rate, and two or four streams in MIMO transmission'	'To investigate the effect of different experimental environments on Wi-Tar performance, we conducted identical experiments in three different indoor environments. As shown in Fig.12, different materials can be identified with more than 99.5% accuracy in all environments, and different liquids, metals, and ordinary objects can be detected with more than 99%, 99.3%, and 99.1% accuracy, respectively. The above results demonstrate that Wi-Tar, which exhibited excellent performance in all indoor environments, possesses good robustness.'	'We find that the reflected channel response is greater when the target object is close to the central line between the transmitter and receiver, where strong reflection is usually incurred by the object. Moreover, as shown in Figure 9(a) and (b), both the width and position of the target object hidden in the baggage or box can be clearly identified from the reflected CSI amplitude (e.g., red color). Furthermore, when there are multiple objects in the same baggage, such as the metal object together with clothes as shown in Figure 9(c), the metal object dominates the reflection signals and can still be distinguished and imaged.'	'The reason is that PC1 of the unoccupied room has high variation which reduces the overall signal to noise ratio of the occupied and unoccupied rooms. As an example, Figure 8 shows the temporal fluctuations of PCs 1 and 2. PC1 indicates a signal with multiple levels whereas PC2 consists of a single level. We argue that these multiple levels are a result of multiple peaks and valleys of the CFR caused by frequency selective fading'	'Before collecting offline data, we first need to establish a reasonable distribution of indoor measurement points. We divide the ground equally into 32 1 m × 1 m areas outside the occupied area by table and chairs. The center of each area is set as a measurement point; AP and MP are placed on two sides of the scene as shown in Figure 6. Considering the fact that the impacts of different target states on wireless signals are different, in this scheme, we generate feature fingerprint and determine the state of the scene by comparing the similarity between online and offline fingerprints.'	'In [28], the authors proposed a multi-room presence detection system in which only a transmitter is required, and the number of receivers depends on the number of rooms. With their proposed C-MuRP system, they obtained an accuracy of over 90%. On the other hand, a Wi-Fi CSI based passive human intrusion direction detection system is developed in [29]. They propose an algorithm to monitor changes in amplitude and angle of arrival distributions of reflections and perform human intrusion detection.'	**With more Wi-Fi transmitters and receivers nearby, accuracy increases. It is beneficial if all the devices are on different channels, since multiple devices on the same channel causes interference decreasing accuracy due to overlapping. More Wi-Fi devices allow for more accurate measurements. Open spaces are generally better due to less reflection effects that could distort the signal. Reflected channel responses are greater when the person/ object is placed directly in between sender and receiver.**

Which type of MCUs / sensors are typically used in other research involving CSI-technology to achieve good results?	'We employed a Netgear N300 wireless router and a Cisco RV180W wireless router as transmitters, operating in IEEE 802.11n AP mode and in 2.4GHz band, both having two transmitting antennas, and two computers equipped with Intel Wireless Link 5300 NICs (IWL5300) as receivers, each with three receiving antennas.'	'Currently, the most widely used tool for CSI extraction is the Intel CSI tool in [1]. For the purpose of our experiments, we adopt this Intel 5300 NIC CSI tool and focus our investigation on the CSI amplitude.'	'To further investigate how the sampling rate affects The performance of the proposed methodology, we transfer the system to the traditional wireless platform. A TP-LINK TL-WDR7500 WiFi router that supports IEEE 802.11n standard functions as the transmitter, and a mini desktop (physical size 170 mm x 170 mm) with three antennas works as the receiver. The mini desktop is equipped with an Intel 5300 NIC and runs Ubuntu 12.04 OS. With Linux 802.11n CSI Tool deployed, the mini desktop can collect CSI measurements.'	'To evaluate the performance of PADS, we conduct real experiments on commodity-ready COTS devices. Specifically, we use mini-desktops with three external antennas as AP and client. Both mini-desktops are equipped with Intel 5300 NIC and run Ubuntu 11.04 OS.'	'Therefore, the CSI measuring station is simply based on the WLAN device. However, although a CSI monitoring station requires functions of communication, capture, memory, etc., the impact on total cost is small because there is only a single CSI monitoring station. In addition, CSI can be transferred efficiently since it is possible to apply SU-MIMO and MU-MIMO transmissions and use CSI acquisition stations with multiple antennas to achieve high transmission speed.'	'To implement the proposed Wi-Tar system, we employ a TP-LINK TL-WDR4310 wireless router with OpenWrt firmware version v1.0 as the transmitter. Treat a desktop computer equipped with an Atheros AR9580 NIC as the receiver. The transmitter operates in 802.11n AP mode in the 5GHz frequency band, and the receiver runs Ubuntu 14.04 LTS with a recompiled kernel of 4.1.10+. Both are equipped with an omnidirectional 6 dBi external antenna extension cable with dual-band support. The transmitter sends data at a transmission rate of 200 packets/s, and the raw CSI contains the amplitude and phase of 56 subcarriers with 3 transmitting antennas and 2 receiving antennas.'	'We implement our system on a pair of laptops, which are equipped with IWL 5300 wireless cards and three 6dBi omnidirectional dual band rubber ducky antennas. The two laptops are placed upon a wooden table in a typical indoor room, and we employ two setups as shown in Figure 3 to perform material identification and risk level estimation, respectively. The laptops are running Ubuntu 10.04 LTS with the kernel 2.6.36, and the WiFi card works at 5GHz frequency band with the transmission rate 100pkt/sec. During data collection, two people are in the room standing by the table to imitate the practical scenarios.'	'The transmitter and receiver of the experimental setup consists of two laptops, ACER 5740 and Lenovo Thinkpad L520 Both run Ubuntu version 14.04. Each of them is equipped with three external antennas. We installed a Wi-Fi card with the IEEE 802.11n IWL 5300 chipset, modified driver and firmware in the two laptops to function as the transmitter and receiver in our work. Both Wi-Fi cards in the two laptops were programmed to operate in monitor mode, which is one of the Wi-Fi modes provided by the IEEE 802.11n standard to sniff packets in a particular channel.'	'We use a Wireless Access Point (AP), a wireless router, and a computer with a 3-antenna Intel 5300 NIC (Network Interface Card) as a monitoring point (MP) in a 8.5 m × 5.7 m indoor scene and get CSI data by modifying the firmware. The experimental platform is a Wi-Fi based wireless sensing system platform built by the integrated installation tool (TNS-CSI Tool) based on a "Linux 802.11n CSI Too'	'An Acer Travelmate 6293 laptop with Intel WiFi Link 5300 802.11n wireless network card was used to gather CSI measurements from the access point, which was configured using the Linux 802.11n CSI tool developed by [32]. This laptop has three internal antennas for wireless communication. The CSI tool provides CSI values in a format that reports the channel matrices for 30 subcarrier groups for every two subcarriers at 20 MHz. Each matrix entry is a complex number specifying amplitude and phase of the signal path between a Tx–Rx antenna pair. On the other hand, an ASUS RT-N12E Wireless-N300 access point with two antennas was used.'	**In most studies the Intel 5300 NIC (network interface card) combined with a Linux operating system running on a computer were used for CSI data collection and analysis. The 5300 series NIC cards are widely available and a popular choice for these types of experiments. These network cards can be modified with an open-source custom firmware for CSI collection, like the 'Linux 802.11n CSI Tool' [12]. The router models and brands are different, but they all support the IEEE 802.11n standard, which allows them to use multiple antennas at once to optimise data delivery to receiving devices.**

Methods & techniques

One important aspect of the sensor module is the power consumption characteristics of the system. This is important because one of the main requirements for the system is that it must be able to operate autonomously for extended periods of time. With power storage and power harvesting techniques it is possible to achieve a lot in regard to autonomy, but the energy consumption of the system is also of great importance. If the power consumption is higher than the energy harvesting capabilities, it becomes impossible to operate the system from just the incoming power. This means that a second power source (the energy storage system) has to be used to maintain functionality. This also has as a consequence that it becomes impossible to store more energy in the energy storage system, since more energy is consumed than is harvested. A summary of the power systems is shown in Figure 1 below where the arrows indicate the possible flow of energy.

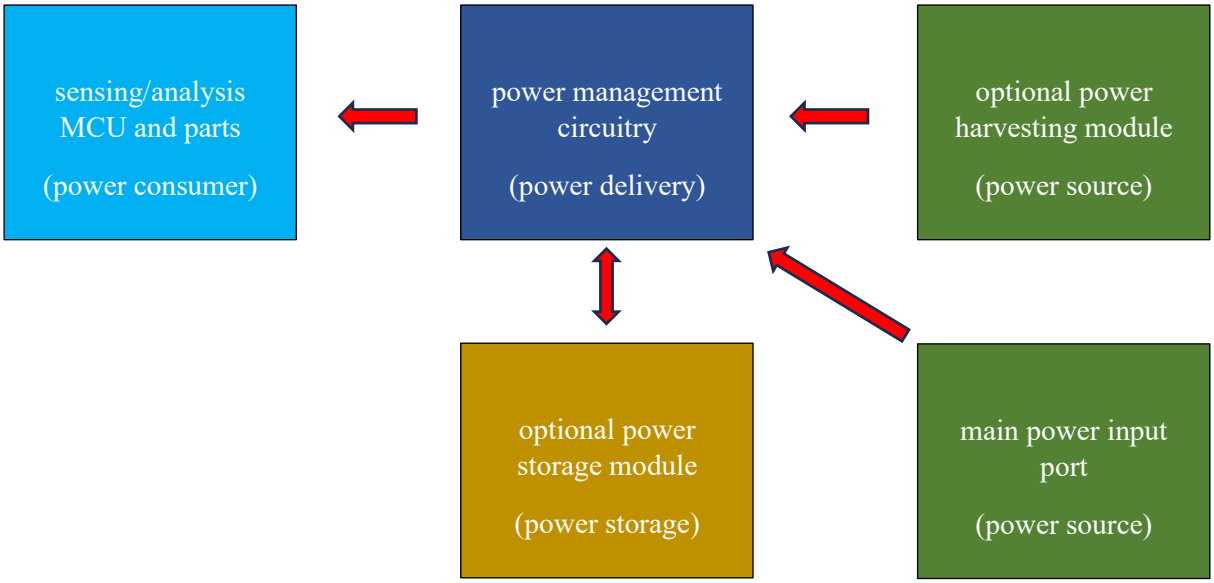

Figure 1: overview of all the energy related parts of the sensor module

In order for the sensing and analysis parts to operate, there has to be sufficient power available in the power delivery circuit for delivery to the power consumer. If this is not the case, the sensor module is unable to execute its given task. It is important to determine how much power is used by the power consumer in order to find out the design requirements for the power source and power storage solutions.

All hardware parts will carefully be selected for their electrical characteristics. Only energy-efficient parts and parts with low leakage currents will be selected. Therefore, the focus of the experiments will be on energy efficiency within software. The MCU that is going to be applied for the sensor module is the ESP32. This MCU is known for its many capabilities, but also its high energy consumption when active. Luckily, the ESP32 offers various methods to save on energy consumption in software. Internal parts of the MCU can be disabled with different sleep modes, and output RF power can be turned up and down to save on energy usage.

A possible method for making the sensor module work autonomously 24 hours a day is to disable the sensing and analysis part during the day while harvesting energy with solar panels. This energy can then be stored and used at night. To test the feasibility of this idea, it is important to know how much power is still being consumed when the sensing parts are disabled, and how much when enabled. This information is crucial to determine if the energy harvesting module could be sufficient to charge the energy storage solution (lithium-ion battery) during the day and drain it during the night.

Other than the power usage experiment, there will also be an experiment conducted to verify that the MCU chosen for this project (ESP32) is suitable for CSI analysis applications. According to the literature research, many CSI-based projects are made using a computer running an operating system (Windows or Linux) with a NIC (Network Interface Card). The NIC is often then flashed with a custom firmware which allows for detailed CSI analysis that would otherwise not be possible on the native firmware delivered with the hardware.

Due to the requirement of a low-power CSI analysis sensor module, using a real computer using an operating system is not feasible. Even though low-power computer systems exist with an energy-oriented operating system, computers will never be able to beat the efficiency characteristics of a dedicated MCU that only runs the software which is strictly required.

There are many microcontrollers and SoCs available from various manufacturers and at different price points. All of these options have their own benefits and drawbacks. When it comes to the development of a project, not only hardware specifications are important. When there is already software available for a particular problem, it is convenient to base the project on this platform to speed up the development process and to increase the chances of success when doing the validation experiments.

An example of a software package that is already available for a common-used MCU is the ESP32 CSI Toolkit [14]. This is a software package that was written for the ESP32-series of chips manufactured by Espressif Systems. The toolkit allows for easy CSI data collection, both active and passive. With the change of a few parameters in the setup the configuration can be altered to suit the needs of the user. Because of the availability of this software and its ease of use, it becomes an interesting candidate for the sensor module. The hardware that it is running on (ESP32) is also a relatively cheap and widely used microcontroller. This makes the hardware design process easier since there is a lot of documentation available.

To verify if the software works as intended for the ESP32, experiments need to be conducted. If this software proves to be a convenient way to do CSI analysis on relatively cheap and energy-efficient hardware, the ESP32 microcontroller can be applied for the purpose of creating the sensor module.

For the experiment, the active CSI collection method will be utilized. This is the mode where two ESP32 chips are used to generate Wi-Fi traffic between the two nodes. Due to this generated traffic, there is a constant stream of data packets over WiFi, which makes CSI collection consistent and more reliable. This mode is the best way to conduct the experiment, since it is always certain that CSI data is generated and collected. The data can be analyzed to check whether there are people or objects in between the two nodes.

Even though the final implementation will be able to use active CSI sensing as well as passive CSI sensing, experimenting with active CSI sensing only will be sufficient to test the feasibility of CSI sensing in general for the ESP32 microcontrollers. The passive CSI sensing method works the same way as the active sensing method, but then with the requirement of external network traffic by APs and clients. For the sake of setup simplicity of the experiment, it is better to use active CSI sensing for this purpose.

The setup for both experiments will be described in the following setup descriptions. Experiment one and two are related to the power consumption of the system under various settings and conditions, and the third experiment is to test the feasibility of CSI sensing on ESP32 based systems. After the experiments have been conducted, the results will be reviewed and analyzed further into clear conclusions with the purpose of aiding with the design process of the sensor modules. The practical experiments are intended to verify the theoretical assumptions that have been made for the design.

Experiment setup: energy characteristics

The setup shown below in Figure 2 is the baseline setup for both experiments that will be conducted in order to get a clear impression of the energy characteristics of the ESP32 MCU. A development board with a 0-ohms resistor between the power source and the ESP32 module will be used. To measure the current flow towards the ESP32 only, the 0-ohms resistor will be desoldered and a current probe will be placed in series with an ESP32-WROVER module. This experiment is being conducted on a WROVER module (with both flash and PSRAM memory) because the results can then be treated as a 'worst case scenario'. If it is decided in the final design that the ESP32 variant with additional memory is required, the measurements are already valid. If a simpler version is chosen, the power consumption can only decrease. By doing a measurement over the ESP32's power supply net only, all the other components (like LEDs, the USB-to-Serial converter, and the EEPROM chip) mounted on this particular development board.

Since the output voltage of an LDO (Low-dropout regulator) stays constant when the maximum current pull is not exceeded, only the current will be measured during each experiment. Before the experiment, it was confirmed that the output voltage of this LDO is exactly 3.30V, the voltage that it should be at. The power consumption numbers are calculated with the value of 3.30V in mind without taking new measurements for each separate current measurement. The internal brownout detector of the ESP32 has been disabled for the experiments since the internal resistance of the multimeter can sometimes cause the input voltage of the ESP32 to drop under the brownout voltage for a very short time. When the brownout detector is not disabled, the ESP32 will keep bootlooping.

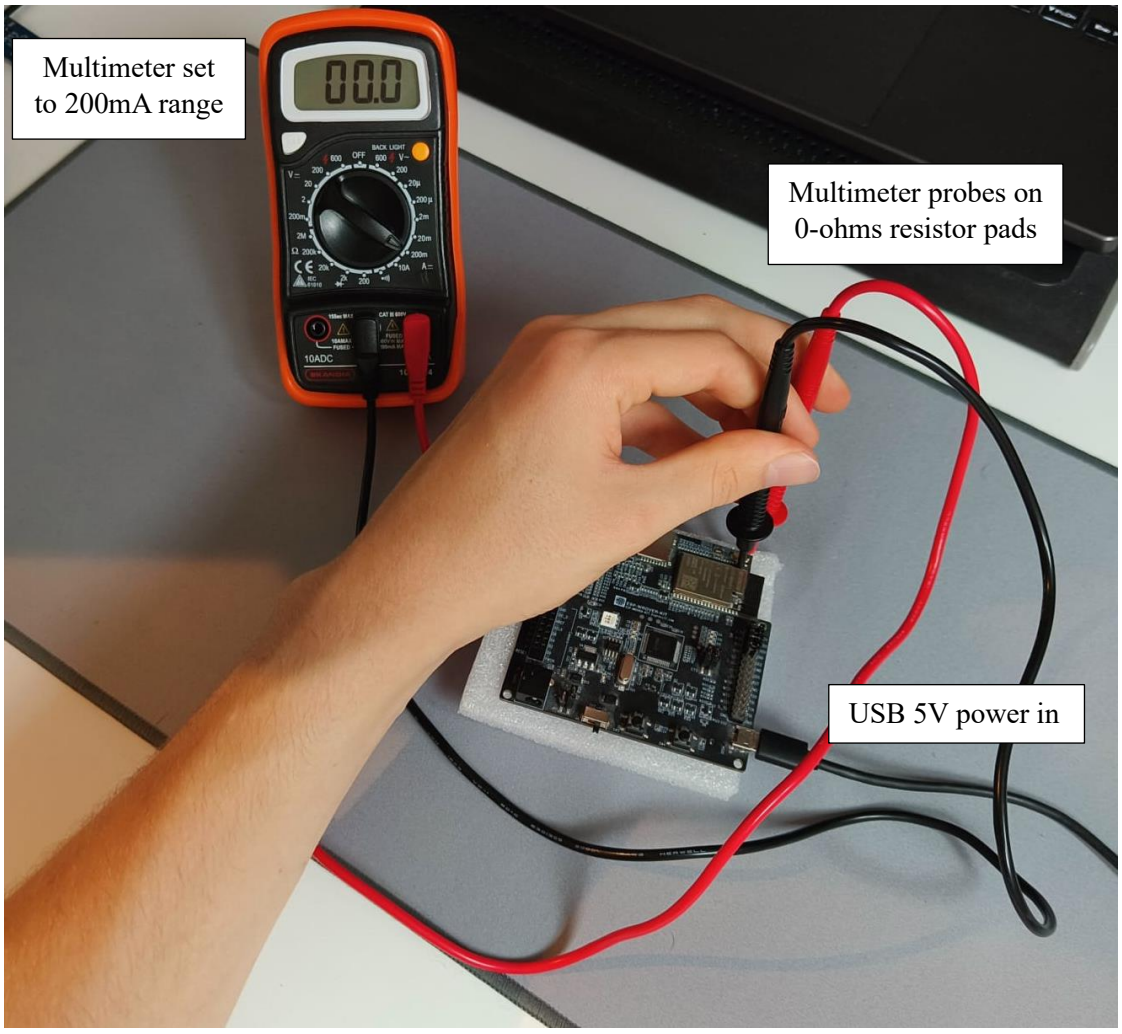

Figure 2: schematic view of the experiment setup

Experiment setup: ESP32-based CSI sensing

A sketch of the physical experiment setup will be shown below in Figure 3. The ESP32 development boards flashed with the right programs will be set up along a quiet road on the university campus. The boards are placed across from each other so the line of sight between the two nodes is a diagonal. When participants walk or cycle through this line of sight, a significant variation in CSI data output should be visible. When this change in the output data is visible, it is apparent that the ESP32 is an excellent choice for the application of CSI data collection. The length of the diagonal line between the two nodes is 8 meters. Cyclists and pedestrians can cycle or walk over the road as usual and the system should be able to pick up these activities and report back on them on the analysis PC.

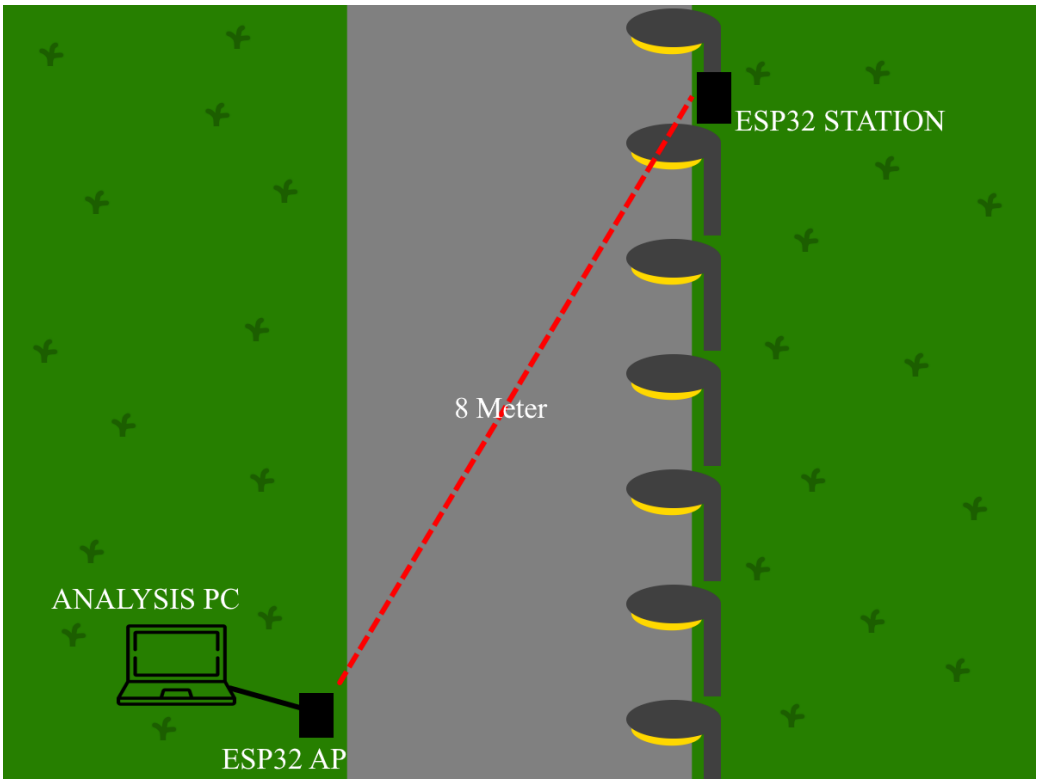

Figure 3: outdoors CSI experiment setup with two ESP32 boards

The exact location of this experiment will be on the University of Twente campus along a road that has been temporarily blocked due to construction work at the time of this experiment. A satellite image sourced from Google Maps of the road can be seen in Figure 4 on the next page. The two ESP32 boards are also mentioned as dots, and the line-of-sight diagonal is also drawn onto the image. The exact GPS coordinates of this area are 52.23909248565892, 6.859322369507232 in numeric format. This road is particularly selected for its lack of traffic during the experiment. This makes it possible to isolate the data from the participants, as they are the only traffic that is recorded. The fact that it is a straight road is beneficial for the experiment, this makes setting up a line-of-sight diagonal along the road easier.

The ESP32 board at the streetlight will be programmed with the Active CSI Station mode code, and the board at the other side of the road (on the bench next to the laptop) will be programmed with the Active CSI AP mode code. This board will also be connected via a serial-over-USB connection to a laptop with Windows 10 as its operating system, running the recording software provided by the ESP32 CSI Toolkit. Timestamps are added by the software to compare the results with the actual events later. All the data collected by the access point ESP32 is saved to the laptop in a .csv file for analysis later on. The ESP32 configured as station be placed 30 centimeters of the ground on top of a backpack, and will work of a USB power bank inside of the backpack.

Figure 4: satellite image of the testing area with the indicating the locations of the ESP32 boards

The access point is set to advert a Wi-Fi network with the SSID set to 'CSI AP' and the password set to 'ESP32Experiment'. These variables can easily be changed within the code the toolkit provides by running the command 'esp.idf menuconfig' in the ESP-IDF terminal window. This brings up a GUI which allows the programmer to change several parameters in the stock configuration of the ESP32 CSI Toolkit. The password is configured in order to prevent other users from (accidently) connecting to the access point, potentially invalidating the research results. Both boards will be configured to the same Wi-Fi channel (channel 6+10). Also the channel can be configured with the configuration GUI mentioned.

The ESP32 supports two bandwidth modes for Wi-Fi channel selection, HT20 and HT40 (20MHz and 40MHz bandwidth respectively). To ensure a high data throughput and due to the lack of other Wi-Fi devices nearby that can cause interference, HT40 (40MHz) bandwidth was chosen. After a quick scan of the environment of the test setup, channel 6+10 was chosen due to the lack of other transmitters on this channel in the same area. This ensures that only packages from the other ESP32 are collected and analyzed, without the interference of other nearby Wi-Fi capable devices. A screenshot of the channel analysis can be seen in Figure 5 on the next page. It might seem like there are a lot of other devices on channel 6 already, but due to the 6+10 configuration, the average transmitting frequency is actually at the same frequency as channel 8, which is completely empty.

The ESP32 set to station mode will be used to transmit packages to the AP. The output data will be sent over the serial port of the ESP32 configured as access point, and will later be further analyzed after the laptop running the collection software that comes with the toolkit has collected all the experiment data. The code for both ESP32 boards is compiled with version 5.0.4 of the ESP-IDF. This is due to a known issue with CSI data collection in combination with newer versions of the ESP-IDF. Compiling the code with the incorrect version will result in a crash due to an issue with the priority setting of a task in the FreeRTOS system. At the moment of this writing, Espressif Systems is still working on a fix for this issue. Therefore it might be possible that future versions of the ESP-IDF will work without any issues. Out of necessity, this project will use a slightly outdated version of the ESP-IDF.

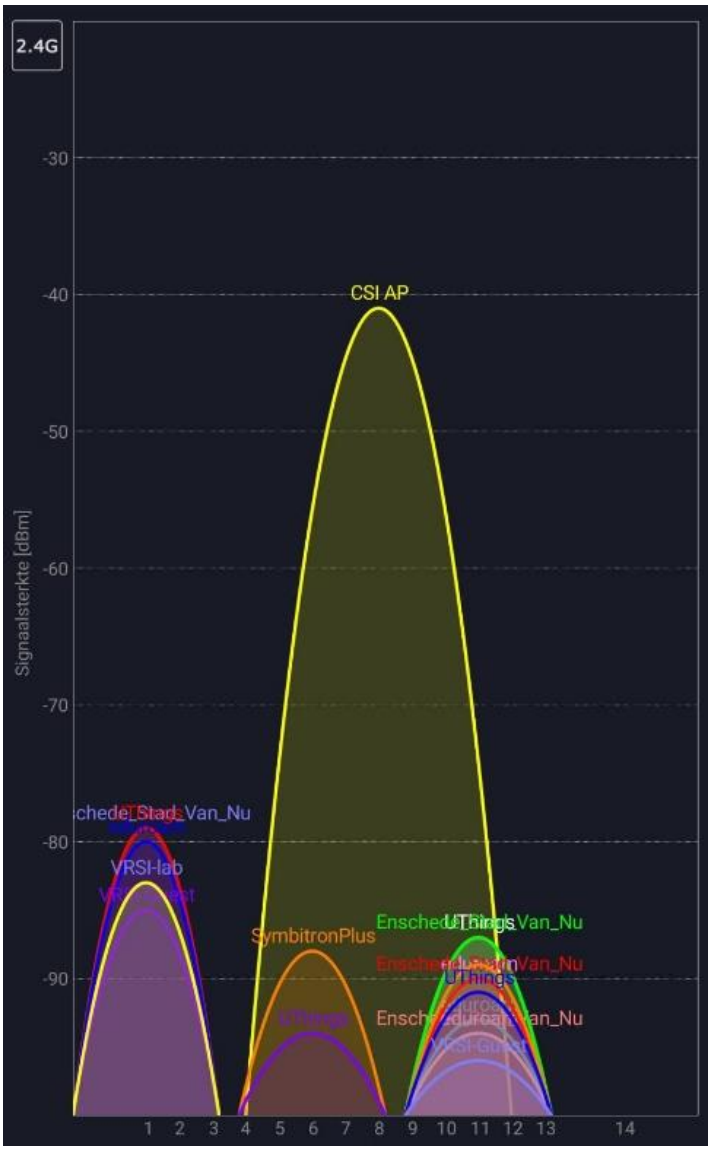

Figure 5: Scan of available Wi-Fi networks and their channel on the experiment location.

Several pictures of the experiment setup were taken, these pictures can be seen in Figure 6. Higher resolution pictures can be found in Appendix 1.

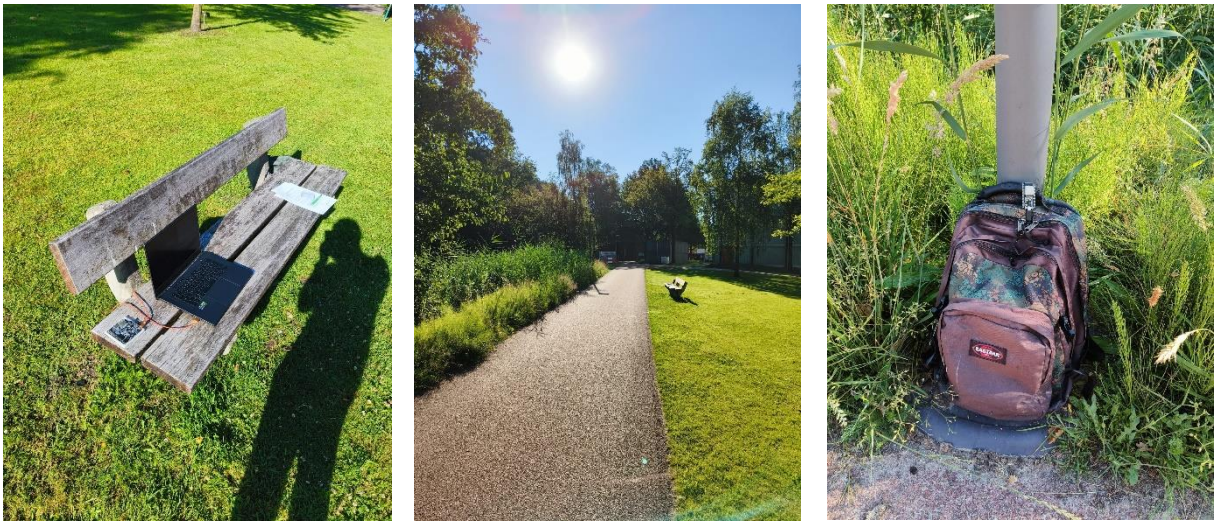

Figure 6: Picture of the AP ESP, the experiment road, and the station ESP32 (left to right)

Ideation

For this project, the end user group was decided to be individuals working with CSI data on a regular basis, like developers and researchers. The design process started by collecting the requirements of the end users which would assist them with their work. An interview was conducted with one individual which had done a lot of research in the field of CSI data analysis already. Several meetings were set to discuss the requirements of this individual, as their design requirements would be representative for other people active in the same field.

The most important design requirements which are currently missing in off-the-shelve solutions were collected during these interviews. The following requirements resulted from those interviews:

- ESP32 as the main microcontroller (easy to develop for, large user base, open-source code already available, powerful, versatile)
- Possibility to connect multiple antennas to the board and to switch between them (allows for multi-directional analysis and to compare different antennas easily)
- Additional non-volatile storage for storing CSI data
- Easy USB interface for programming and data collection (an interface which allows for updating the firmware of the board which is also fast enough to output real-time CSI data to another device over the USB port)
- Possibility for the board to operate stand-alone for long periods of time without human intervention (which means no direct connection to an additional device or power source)

With these design requirements in mind, specific parts were selected for the board. For the first design requirement, the product finder on the Espressif Systems website was used to select the best SoC for the application. The selection to choose from only included SoCs and no modules. This is because another requirement is the possibility to connect multiple antennas, which is not possible using a module because all modules have integrated antennas or a single antenna connector.

To accommodate for the requirement to connect multiple antennas to the ESP32 SoC, an additional part needs to be selected. The ESP32 only has one single RF port, so in order to connect multiple antennas which are individually selectable an RF switch needs to be added. In selecting an RF switch, there are a few specifications especially important. The specifications of most importance are the insertion loss at the operating frequency (2.45GHz), the number of antennas that can be added, and the impedance of the input and the output antennas. Choosing a part that is fairly-priced and widely available is also beneficial for when the design is put into production. This is why the JLCPCB parts library was used for choosing the perfect RF switch.

For selecting the additional storage chip the same JLCPCB parts library was used. Because CSI data needs to be written to memory quickly in order to be ready on time to receive the next incoming packet, a high-speed memory solution is absolutely essential. Memory using the SPI protocol is the only realistic option for this purpose since it allows for speeds up to 40MHz with the ESP32. Due to the excellent speed performance and durability ratings, FRAM memory was chosen. FRAM is considered a niche memory technology by most people, but for speed-critical applications in which durable and non-volatile memory is required it is the best choice.

Because of the need for a device that is able to operate stand-alone, special care needs to be taken in designing the power system. The system must be able to operate without direct access to power. It also needs to be able to supply all the parts on the board with sufficient power to operate.

The only realistic solution for storing large amounts of power are lithium-ion rechargeable batteries. These batteries offer energy densities not yet achievable by other cell chemistries. Another advantage of lithium-ion cells is their ability to handle large amounts of current, which allows them to be charged and discharged rapidly. A fast discharge speed is not required for this project, since all the components are as energy efficient as possible, but fast charging when connected to a charging cable is practical when doing a lot of research with the same board.

For power harvesting when there is no electricity source nearby, solar panels were chosen to be the best option. Solar panels offer the highest energy yield in outdoor environments compared to other techniques. Since one of the target applications of the board is outdoor usage, an energy harvesting technique that can operate outside is essential. Due to the electrical characteristics of solar panels, using a MPPT (maximum power point tracking) algorithm is essential for harvesting the most energy. In Figure 11 below, a typical IV-curve of a solar panel is shown.

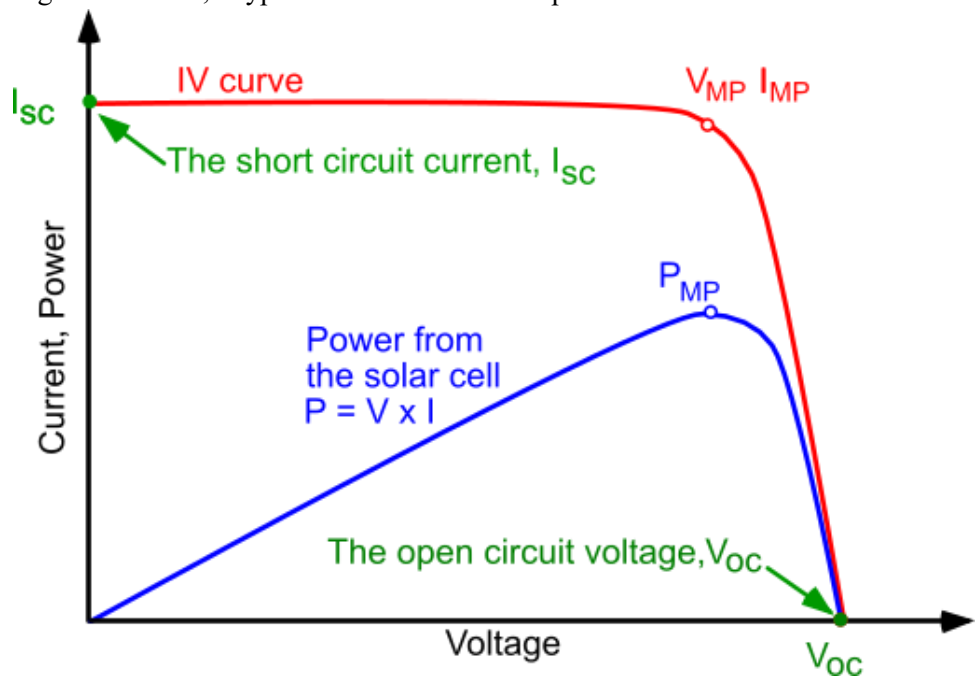

Figure 11: typical IV-curve of a solar panel [15]

As can be seen in the figure, due to the shape of the red curve the power curve shown in blue has one single point with the highest amount of energy. This point needs to be traced with electronic circuitry in order to deliver the highest amount of power given the circumstances.

Many integrated circuits already exist for the purpose of tracking the maximum power point with MPPT algorithms. These chips have a specified maximum voltage and current, and are able to track the maximum power point of any solar panel within the given boundaries. This gives a lot of flexibility to use any solar panel available that matches the specifications of the chip. To find the perfect integrated circuit for this application, the JLCPCB parts library was used once again to compare all the available offerings in this specific field of products.

Once all the important parts were selected, schematics were created using free and open-source software called EasyEDA. This program allows its users to create schematics using the part library of JLCPCB. A screenshot of the schematic of the board can be seen in Figure 12. Once a schematic is completed, it is possible to convert the schematic to a PCB with the same software. All components will then be copied to the board with all the connections that need to be made indicated with ratlines (small lines between the pads of components that need to be connected). This feature makes it easy to connect all the pads together with copper traces according to the schematic.

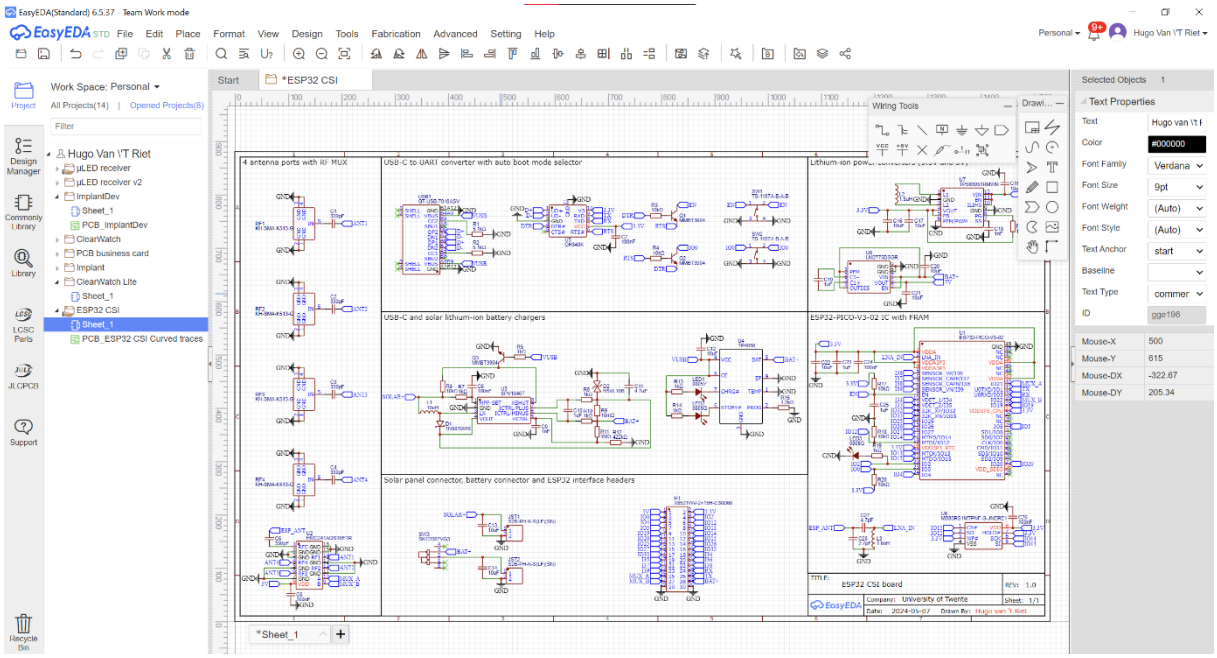

Figure 12: screenshot of the schematics editor in EasyEDA

The schematic created with the parts selected using the design requirements was then converted to a PCB design. A screenshot of the PCB editor tool can be seen in Figure 13. During the design process, special care was taken for designing the parts which involved RF. RF signals are of a high frequency and are therefore very susceptible to poor circuit design, which can lead to reduced performance. Instead sharp corners, all traces involving RF were designed to be smooth and curvy. Vias are placed along the RF traces which connect the two ground planes together. This isolates possible noise coming from the RF lines which can influence the rest of the circuit, and switching noise from other digital parts from degrading the RF performance.

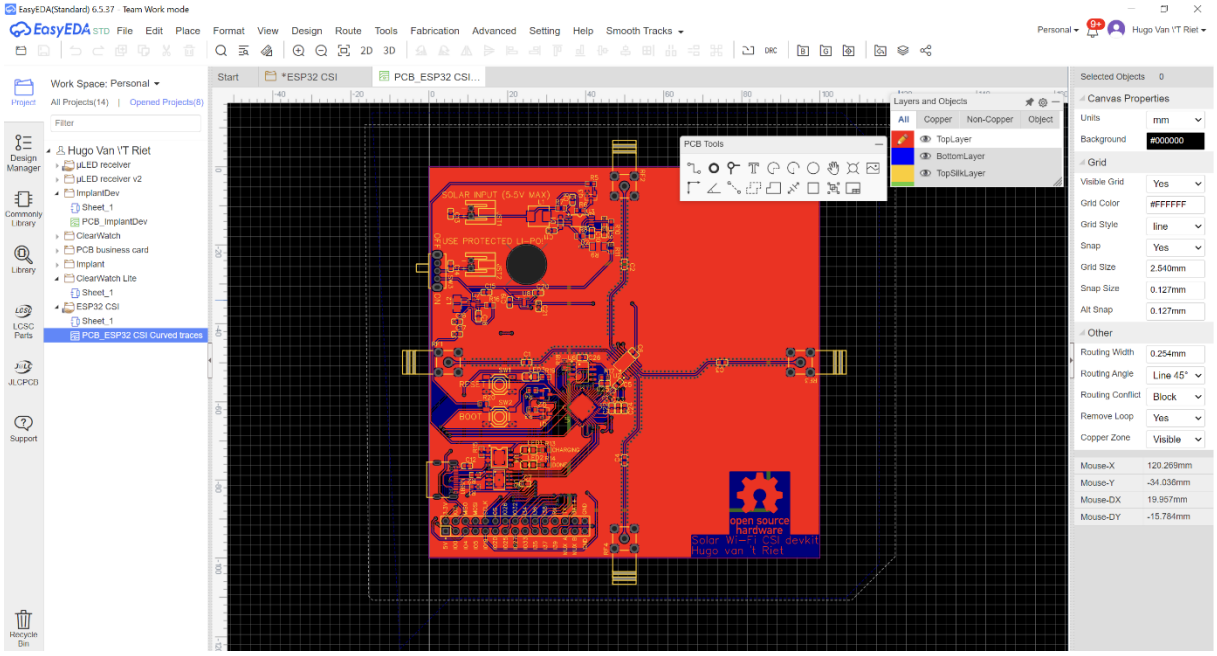

Figure 13: screenshot of the PCB editor in EasyEDA

The project was shared on the website of OSHWLab at the following URL: https://oshwlab.com/hugovantriet/esp32-csi. The project can be inspected on this site. This allows people to inspect the hardware first before they decide on if they want the board or not. Currently there is not yet a ready-made board that can be ordered, but updates will follow on this site.

Specification

Parts:

The particular ESP32 SoC of choice for this board is the ESP32-PICO-V3-02. This is a recent version of the ESP32. The advantage of this particular model is that all the storage and memory is integrated into one package, which eliminates the need for an external memory solution. It has built-in flash memory (8MB) and PSRAM (2MB). The large flash memory is useful for developers to fit a large program onto the chip, and the additional PSRAM can be useful for doing complex calculations which need a lot of temporary memory. The clock crystal is already integrated, as well as most of the required passive components. This makes using this chip very convenient, and allows for a more compact board design. Because this is a recent version of the ESP32, it has the V3 silicon revision. Earlier versions of the ESP32 used to have small design mistakes in the silicon wafer design which introduced bugs. Because these were hardware mistakes manufactured into the silicon wafer, there was no real solution for these issues. With this chip having the V3 silicon revision, there are no known bugs in hardware as of this writing. This allows developers to use the ESP32's full potential without issues due to the hardware.

Because all ESP32 ICs have just a single antenna input/output channel, and multiple channels is required for accurate CSI analysis, the board will include an antenna MUX switch. The switch will be responsible for routing the single antenna channel of the ESP32 to all the different antennas present on the PCB. Most RF MUX switches only offer two antenna output ports, but there are several models available, like the HMC241AQS16ETR by Analog Devices. This particular MUX has one RF input, and four RF outputs that can be selected. Choosing one single MUX solution instead of multiple two-channel MUX switches increases efficiency because there is no need for impedance matching circuits that reduce the signal levels. The MUX can be controlled by the GPIO pins of the ESP32, making it possible to program the best moment to switch the antenna direction and position. Impedance matching networks are added just to the input and to all the outputs of the MUX switch, for optimal performance and minimal signal loss. The datasheet suggests that the typical switching time for this MUX switch is just 40 nanoseconds. The ability to switch between antennas very rapidly is a useful characteristic for CSI technology, since the antenna must be fully switched before the next packet is coming in.

For the FRAM memory discussed earlier, the MB85RS1MT FRAM chip by Fujitsu was chosen. It offers a relatively large storage size of 128 kilobytes at high reading/writing speeds. The maximum operating frequency for reading from this memory is 40MHz. This is very fast for a single SPI connection without the usage of Dual and Quad SPI modes. Fujitsu guarantees that the memory will not stop working due to writing fatigue until at least 10^{13} write operations have been executed. This memory also offers various power saving features for when the memory is not used. When put in sleeping mode, this memory only consumes a maximum amount of 10µA. This memory can be used to store data that must be retained when the device power-cycles. The fast writing speeds allow for real-time CSI data recording in this memory chip. The high endurance rating is essential since CSI data typically comes in at high speeds, so overwriting the memory will happen often in order to record the last few frames.

The ESP32 cannot communicate with a computer over USB by itself, this generation of the ESP32 does not have native USB support like the ESP32-S2 and ESP32-S3. Because of this an external USB to UART converter is required for 'translating' the communication between a PC and the ESP32. The chip chosen for this purpose is the CH340K. The CH340 series of converters is often used, and therefore has excellent driver support for all platforms. The K variant of this series was chosen due to the amount of the chip package. It offers only the basic pins required for UART communication, plus the additional DTR and RTS pins. These pins are used to auto-reset the ESP32 and to put it into boot mode when new firmware is being flashed. This is more convenient for the user.

An automatic reset and boot mode circuit is included, but control buttons for these pins are still included for manual operation if required. The boot button can also be used as a user input once the ESP32 has booted into the firmware already. The CH340K supports baud rates up to 2 megabaud, this allows for very fast communication between a computer and the board.

For charging a 3.7V Lithium-Ion polymer battery connected to the board, there are two on-board charging techniques. The first one is the TP4056. This chip is a dedicated Lithium-Ion battery charger with constant current and constant voltage charging modes. Lithium-Ion cells require a charging voltage of 4.2V. The USB port input voltage is around 5V. This means that about 0.8V needs to be dissipated in order to safely charge Lithium-Ion cells. This is done on the TP4056 itself which saves additional external components on the board. The maximum charging current can be programmed by setting a resistor value on a programming pin. On this board the charging current has been set to the maximum allowed by the TP4056, which is 1A. Two LEDs are connected to the chip to indicate when the battery is charging and when the charging process has been completed. The TP4056 includes a temperature sensing feature to stop or reduce charging when an overheating event has been detected. Since the battery can be chosen and installed by the user, the temperature sense feature offered by the TP4056 has been disabled. If the temperature sensor is placed in the wrong location, it could possibly hinder the charging process. The maximum charging current is only 1A and all batteries used with the board must include an on-battery safety circuit, therefore it is safe to disable this feature.

An alternative charging option is by using the power harvesting solar panel circuit. To get the most amount of possible energy out of the solar panel, the SPV1040T solar charging chip was chosen. This solar charger has a built-in smart MPPT algorithm for finding the maximum power point on the solar panel IV-curve under all circumstances and conditions. The chip accepts input power from 0.3V to 5.5V. Due to this wide voltage input range, the voltage must be eighter stepped up or stepped down. The SPV1040T includes an internal buck-boost converter to make sure that it always delivers the 4.2V required to charge a lithium-ion battery. When USB power is detected, this chip will automatically be disabled. Using a chip that supports MPPT like the SPV1040T is essential for harvesting the most amount of energy as possible.

For both the lithium-ion battery and the solar panel, JST-PH male connectors are used on the board. The polarity of the parts is printed on the silkscreen layer of the board, so users know which type of batteries and solar panels are compatible. Most batteries and solar panels in the industry use the same JST-PH connector, so using these male connectors should allow users to combine the board with any lithium-ion battery or solar panel they want, as long as they comply with the electrical characteristics set by the board. Lithium-ion batteries used should be able to charge at 1A and must be single cell (3.7V nominal cell voltage). Since the board does not include any protective circuitry for overcharging or undercharging the lithium-ion battery, a battery with integrated protection circuitry is required for this board. When a lithium-ion cell is discharged below 3V, it can get permanently damaged. This is why it is important that the protection circuitry is present inside of the pouch cell package itself. The solar panel should have a maximum voltage output of 5.5V since this is the maximum rating of the solar panel charger chip.

Pin headers are placed at the edge of the board to allow developers to create custom hardware additions, and interface them with the board. All the unused GPIO pins of the ESP32 are routed to these headers, they can fulfill any custom functionality if the application requires it. Some of the important pins of the development board itself are also routed to these headers for analysis, battery voltage for example. It is possible to externally read the charge status of the battery by measuring the voltage. Also the MUX input pins are broken out, so it is possible to switch the antenna connected to the ESP32 externally. Power to the board can also be provided using these pins instead of the normal USB port. The main function of these pin headers is to add flexibility for those developers and applications which require additional features that are not offered by the board as standard.

PCB design features:

The board is equipped with four antenna sockets typically used for 2.4GHz screw-in antennas. These sockets are placed in the middle of the four edges of the board. This is done to make sure that the distance between all antennas is equal. The possibility to use multiple antennas allows for the usage of directional antennas which all cover a certain angle. With these directional antennas it is possible to see where a CSI data packet is coming from. When the approximate direction of the packet can be determined, it is possible to do a more in-depth analysis of the source of the package. This has the potential to make position estimation even more accurate and precise.

For traces used for RF applications, it is usually recommended to make sure that there are no sharp corners in these traces. If there are sharp corners, the signal can become degraded due to the trace design. This is because RF signals are of a high frequency. High frequency signals behave differently than standard DC signals. The board was designed with these characteristics in mind. Design advise for high frequency applications was taken from the website of Sierra Circuits, a PCB fabrication company. The website [16] indicates that a few design choices are essential for a good high frequency tolerant design. One of the most important requirements is to only use one single copper layer. Using vias to go to another layer is not recommended since vias can add parasitic capacitance. Another important characteristic of high frequency traces is to use the least amount of bends as possible, straight lines are the best for these signals. If bends are still required, circular bends are much preferred above angular bends. Vias to connect the ground planes together along the high frequency traces reduce parasitic inductance caused by ground return paths, so these vias were also placed along the RF traces on the board. The RF MUX switch chip is placed in the center of the PCB with a rotation of 45 degrees. Due to the pinout of this chip, it was possible to make the traces to all antennas approximately the same length when rotating the chip to this 45 degree orientation. With the trace lengths of all RF signals being very similar, it is easier to compare incoming signals without compensating for additional losses for some antennas while other antennas do not have the same losses. On all the RF traces filtering capacitors are placed to ensure that only a clean signal reaches the MUX and antennas. The values of these capacitors are recommended by the manufacturer of the RF MUX switch and are noted in the datasheets. Further impedance matching is not required for these traces, since the ESP32 has already been tuned for an impedance of 50Ω, as well as the MUX switch and the antennas that can be screwed into the sockets.

The size of the board is based on the form factor of a recommended solar panel and battery. Users are free to adapt these two parts to their own application, but the design was adapted to fit the recommended parts. A hole is placed close to the battery connector. This allows for the battery to be mounted underneath the board while the connector can still pass through the board to connect to the connector on the other side.

All the component codes are printed on the silkscreen layer of the PCB. This makes it easier for developers to compare their boards with the schematics to see what each individual component is doing, and how the components are interconnected. Next to the pin headers there is also printed text which indicates the function of every pin. This makes prototyping on breadboards easier, since now developers do not have to look up the function of a specific pin in the schematics or documentation before using it. The communication pins of the FRAM memory have also been broken out to these pin headers. This allows the external reading of this memory chip, which can be useful for data collection applications.

A simple switch was added to the design to make it easy to disconnect the battery from the rest of the system without plugging out the battery. The system remains programmable and readable since this switch is not connected to the USB 5V input. The switch is only responsible for disconnecting the battery from the rest of the system.

Realization

Experiment one: measure current consumption in active mode

The first experiment will be used to set the baseline power consumption characteristics under several different RF configurations. The ESP32 supports a custom RF output gain selection in order to conserve energy if required. These gains are selectable in software and change the power consumption of the ESP32 significantly. The experiment will be executed by uploading experiment code to the ESP32 where it connects to a Wi-Fi access point and will create its own Wi-Fi access point simultaneously to simulate an intensive task with Wi-Fi. The currents will then be measured for the set RF power parameters, and then the parameter is changed and the code is uploaded again. The table that is going to be filled in during the experiment is shown below in Table 1.

Set RF gain (dBm)	**Current consumption (mA)**	**Power consumption (mW)**
19.5		
19.0		
18.5		
17.0		
15.0		
13.0		
11.0		
8.0		
7.0		
5.0		
2.0		
-1.0		

Table 1: experiment one measurement table (power consumption is calculated after measurements)

Experiment two: measure current consumption in various sleep/suspension modes

The ESP32 chip offers various sleeping modes and methods in order to save power for energy-efficient application like the one being designed in this project. The manufacturer claims that the ESP32 chip can save significant amounts of power by disabling certain parts of the internal processor. This experiment aims to test if the claims of the manufacturer are accurate, and if the same results given by other experiments can be achieved with an ESP32 module with additional PSRAM (WROVER modules).

For this experiment, the ESP32 will cycle through all the available sleep modes. The current draw is measured again and collected. The measured values only apply for the ESP32 chip, and not for the entire board. Since the custom board design has other components, it would not be relevant to measure the power consumption of the whole development board. The data collection table is shown in Table 2. In the ‘active mode’ and ‘modem sleep’ modes the CPU frequency is set to the highest clock speed available, 240MHz. The program used in these modes just contains a simple task of printing text over the serial port. In ‘active mode’ the wireless radio is enabled and connected to an access point, but is not actively performing tasks. The radio is set to its default gain of 19.5dBm. ‘Modem’ sleep is not an actual sleep mode, but is defined by Espressif Systems as disabling the wireless radio in software. This task is also included in the experiment’s code.

Sleep mode	**Current consumption (mA)**	**Power consumption (mW)**
Active mode		
Modem sleep		
Light sleep		
Deep sleep		
Hibernation mode		

Table 2: experiment two measurement table (power consumption is calculated after measurements)

Results: energy characteristics

During the measurements of the first experiment, it became apparent that the RF gain does not have a large impact on the constant current consumption of the ESP32. The peak current draw did change significantly for different RF gains. This is why the original experiment was slightly changed to collect more useful results. Instead of the expected constant current, the peak current consumption was measured. Because the constant current pull did not provide any useful insights, the peak current consumption while at different RF gain levels was recorded and filled into the results table. The power consumption in mW is calculated by multiplying the current by the input voltage of 3.30V. The measurements are shown in Table 3 below.

Set RF gain (dBm)	Peak current (mA)	Power consumption (mW)
19.5	155.5	513.15
19.0	153.7	507.21
18.5	152.1	501.93
17.0	135.0	445.50
15.0	132.2	436.26
13.0	123.3	406.89
11.0	120.5	397.65
8.5	120.1	396.33
7.0	119.9	395.67
5.0	119.6	394.68
2.0	117.3	387.09
-1.0	116.6	384.78

Table 3: results of the first experiment

The results are also plotted in Graph 1 below. A non-linear relationship between the RF gain and peak current consumption can be observed. In the lower range of the RF gain options given by the ESP32, the increase in current consumption is not that large. Increasing the gain to 13 or higher does increase the current consumption significantly. The measurements were taken with a multimeter with a limited sample rate, this means that it is possible that the measurements are slightly inaccurate with regards to the peak currents, since the real peak could have been slightly higher depending on when the sample has been taken.

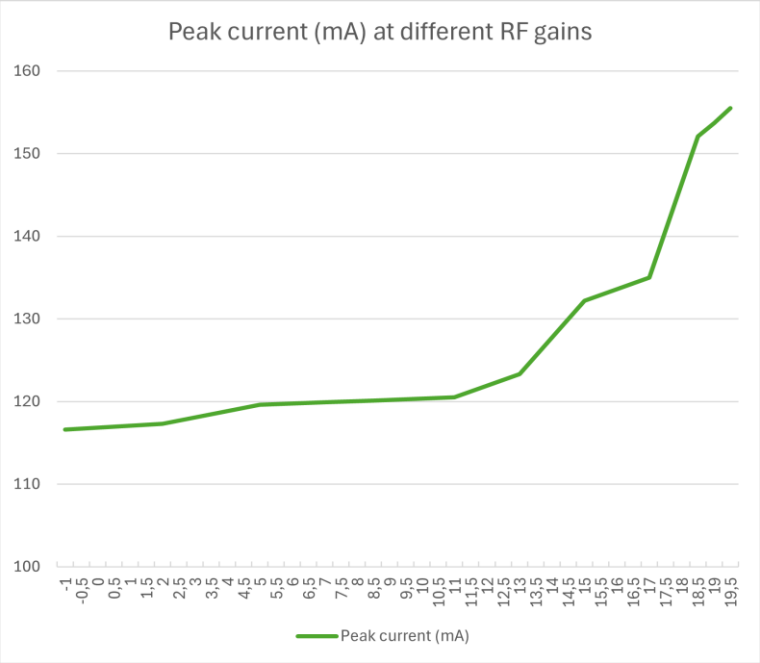

Graph 1: peak current consumption graphed over set RF gain

The results of the second experiment can be seen in Table 4 below. To increase the measurement accuracy, the multimeter was set to the appropriate measuring range for every individual measurement. Due to the significant differences in the power consumption modes the current consumption unit varies for some measurements. Because of this, the calculated power consumption values are also in different units. It can be noticed that the current consumption in active mode is much lower than in experiment one. This is because of the code that was used to test the power consumption. In the first experiment, the ESP32 was programmed to create its own Wi-Fi network as well as connecting to a Wi-Fi access point. Since hosting an access point requires the constant transmission of packages to nearby devices, it is only logical that this consumes more current than simply listening to an existing Wi-Fi access point without actively sending packets back and forth. Therefore the current consumption in active mode is significantly lower in this experiment than in experiment one, even though the RF gain is set to the exact same value (19.5dBm).

Sleep mode	**Current consumption**	**Power consumption**
Active mode	51.2 mA	168.96 mW
Modem sleep	40.5 mA	133.65 mW
Light sleep	1.395 mA	4.6035 mW
Deep sleep	4.81 µA	15.873 µW
Hibernation mode	2.46 µA	7.128 µW

Table 4: results of the second experiment

The measurements taken indicate that the several sleep modes offered by the ESP32 can save significant amounts of power. The ESP32 allows the developer to enter sleep mode duration with microsecond accuracy, making it easy to time exactly when the microcontroller should start sleeping and when it should wake up. Although the modem sleep mode will probably not be very useful for CSI sensing applications (since a constant data flow is required), it can be a helpful mode for when the received data needs to be processed quickly at maximum CPU power (240MHz) without the need for wireless connectivity at that time. Reducing the clock speed can decrease the power consumption further if a high processing speed is not required.

The light sleep mode cuts the clock signal from the two main CPU cores. All the data is kept in memory for when the CPU is connected to the clock signal again. This is an ideal power mode for waiting for a new event to happen on one of the input pins or after some time has passed.

Deep sleep mode disables the main CPU cores, but does allow temporary variables to be stored in the RAM memory of the RTC. This can be useful when some data has to be retained for some time, but the waiting time is too long to keep the powerful CPU cores running. In deep sleep mode, it is also possible to use the UPL (ultra-low-power) coprocessor CPU core. This core is intended to be used for simple operations which are not required to be executed very quickly. An example for a possible use case for this within the CSI data collection field is to use an external IR sensor to see if there are people nearby. When the external sensor triggers, it can wake the ESP32 from its sleep mode. Then a more accurate CSI analysis can be done on where a person stands within a given space instead of just indicating if there is someone within the space.

Hibernation mode is the ultimate power-saving mode. It disables everything inside of the ESP32 except for the RTC, including all the temporary variables. It can use the RTC to wake up the ESP32 again after a set amount of time, or after an input pin has been triggered. This option is ideal for ‘disabling’ the entire ESP32 for a pre-determined amount of time without the need for data retention. After the ESP32 comes back to power, the code will start executing again from the beginning, just like a new boot-up. This mode can be used for letting the ESP32 sleep for a few hours in which it is known that the system is not required to operate. An example of this could be closing hours of a business or office building when it is certain that there are no people nearby to sense. The ESP32 can then automatically wake up the next day.

Experiment three: Active CSI sensing

The time schedule of the experiment session can be seen in Table 5 below. This experiment will be conducted on 26-06-2024 according to the schedule. First there will be a short time where the experiment is set up, there are no participants yet required in this phase. After this, the participants are briefed about the purpose of the experiment and their role in it. Every participant has to sign a consent form before participating, this is to make sure that the data that is being collected is usable for the research and cannot form any negative effects towards the participants. After this phase is completed, the actual experiment can start. After the experiment has been completed, the subjects will be de-briefed with the details how the data is going to be processed and how they can follow further developments of this research (if they are interested). Lastly, all the participants are given a small reward for their collaboration. Since the participants do not have any stakes in this experiment, nor the ability to influence the outcome, it is safe to assume that this reward cannot be linked to changes in the end results of the experiments due to (conflicting) interests.

Timeslot	**Activity**
8:00-8:30	Setting up the experiment, placing nodes.
8:30-9:00	Briefing participants on experiment and the goals, filling in consent forms
9:00-9:45	Experiment taking place, samples/measurements being collected and stored
9:45-10:00	De-briefing of participants, optional

Table 5: experiment timetable of approximated timeslots per activity

Since the experiment is being conducted in the morning, a day with great weather conditions was selected beforehand. This will likely increase the chance that more people are willing to be outside, and are willing to participate in the experiment. Because of this, an increasing in the number of samples that can be taken during the experiment will likely increase.

Participants that are involved in the research will be briefed beforehand about the purpose and goals of this research. They are also asked to sign a consent form (which can be found in Appendix 2). There are no specific requirements for the participants in this research, anyone who wishes to participate can do so. The participants have no interests in this experiment and the results cannot be influenced by participants. This makes the outcome independent of the people that participate.

The task of the participants in this experiment is to walk/run or cycle through the experiment area crossing the imaginary line of 8 meter in between the ESP32 configured as station and the ESP32 that has been configured as an access point. The output data that is generated by the access point board is then sent to the laptop over the serial port, to be analyzed later on. The information is stored separated per experiment in a .csv file, which makes post-processing with a machine learning algorithm quick and convenient.

During the experiments, participants are instructed to follow a particular pre-determined behavior pattern. When the participant starts with their task, the timestamp synchronized to the world clock is taken. This time is also synchronized with the time set on the computer, and so the timestamp attached to the CSI packets also matches this time. This makes analysis after recording easier, since abnormalities in the CSI data can easily be connected to an activity.

A total of 8 experiments are going to be conducted, a short summary of every individual experiment can be found in Table 6. The activities have been selected to match the target application for the developed CSI sensor module, indoors and outdoors activity recognition.

Number	Description
1	Walking participant 1
2	Background CSI data, collected for the purpose of filtering other results
3	Cycling participant 2
4	Walking participant 2
5	Cycling participant 2 & 3
6	Walking participant 2 & 3
7	Cycling participant 3 high speed
8	Walking participant 3 + poses + spin

Table 6: list of CSI sub-experiments with a short description

The analysis done after all the data has been collected is compared to the timestamps placed on the real event. Since the timestamps of the laptop are in sync with the recorded timestamps, it is possible to accurately describe when a CSI package was received, which makes determining if the event has been recorded correctly easier.

Even though this experiment is based on the active sensing code instead of passive sensing (which is also an target application for the sensor module), when the fundamental principle of CSI sensing works for the ESP32, it is safe to assume that it would operate in a similar manner when close to other Wi-Fi emitting sources inside of buildings like Access Points and client devices.

The overall accuracy even has the potential to increase in passive mode, since there are typically multiple APs inside of large office complexes, increasing the number of transmitting sources which makes CSI sensing more accurate. This potential can only be reached if all the devices are tuned at the same frequency (same Wi-Fi channel), otherwise not all CSI packets can be collected since the ESP32 can only focus its radio to one channel at a time.

In order to make sure that all the real activities and CSI detected activities are recorded correctly without of the potential issue of conflicting interests of the main researcher, a second observant is also present verifying all the records and measurements taken by the lead researcher. Both the lead researcher and the second observant will be asked to confirm and sign a declaration that the measurements were taken honestly and with great care, relying on the principle of academic integrity.

Recording video footage of the entire experiment which can be used for experiment result verification by third parties was taken into consideration, but rejected because this complicates the process of finding participants for the experiment. Not everyone appreciates being recorded on video, and by not using video it does not have to be mentioned in the participant consent form, making it easier to find people who are willing to participate.

Results: ESP32-based CSI sensing

The results of all the experiments were stored on the laptop and converted to a graphical representation using several algorithms. The raw data was converted with a moving average filter of 25 frames, a bandpass filter between 0.1-1.5Hz, and a bandpass + moving average filter. Black dotted lines were drawn at the timestamps that were recorded during the experiments when an event happened. This makes analyzing the graphs easier, since there now is a point of reference in time to look for abnormalities within the figure.

The results of all the experiments will be available for review in Appendix 3. In this result section, only the figures of the experiments which returned interesting results will be shown. This approach was chosen due to the goal of this particular experiment, proving that the ESP32 is a suitable microcontroller for (some) CSI based sensing applications. Since the boards which were used were standard general-purpose ESP32 boards, not much can be said about the effectiveness or the accuracy of the ESP32 microcontroller, because the board design was not optimized for CSI applications. However, this experiment can be used to prove that the ESP32 is capable of performing CSI sensing.

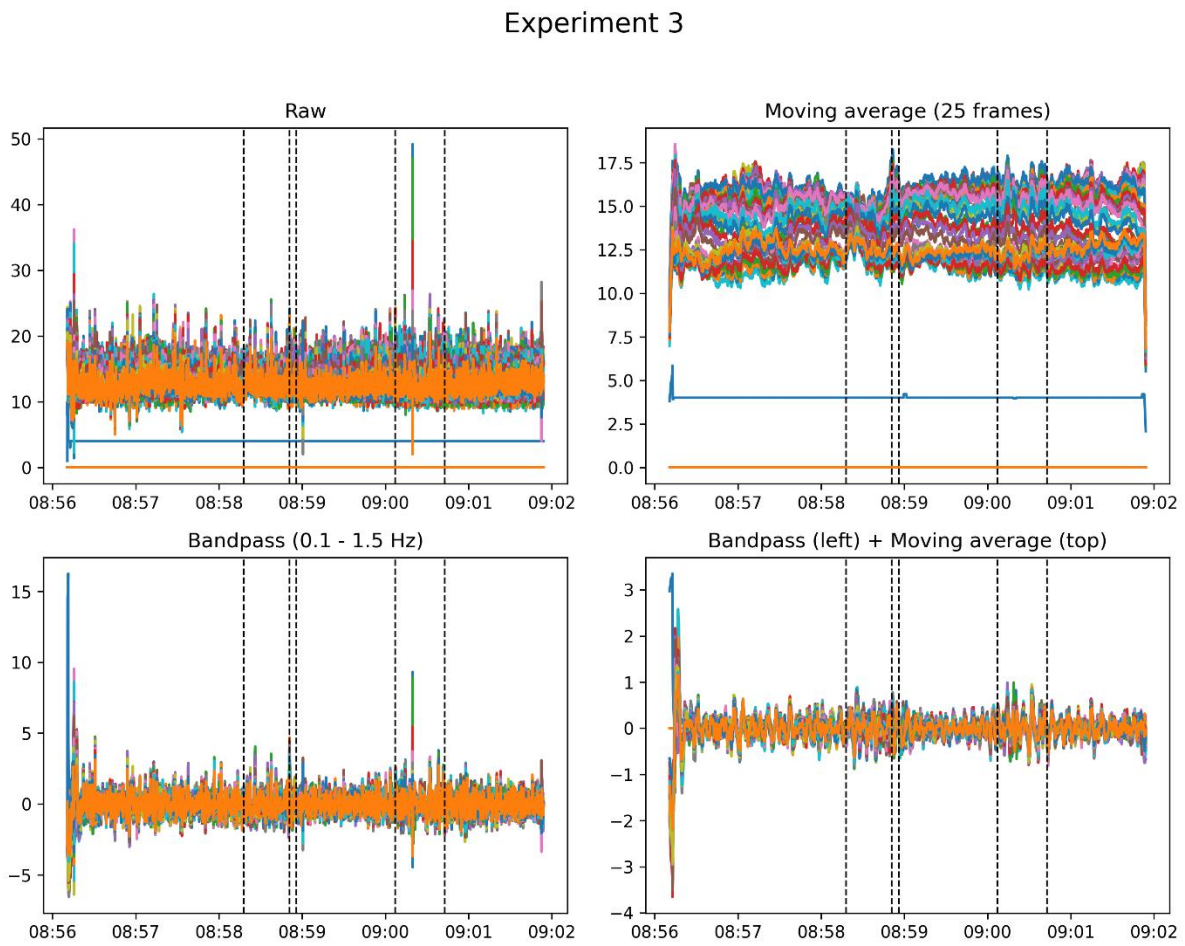

Figure 7: graphical output of experiment 3

The results of sub-experiment 3 are shown in a graphical way in Figure 7 above. This experiment consisted of a test subject cycling through the line of sight, turning around at the end of the road, and cycling back one more time through the line of sight. The timestamps have been added to the figure as well. The first three lines from left to right are the start of the cycling, crossing the LoS, and reaching the end of the road, respectively. The last two timestamps are for starting cycling and stopping cycling one last time while passing through the LoS.

It can be observed that during the two cycling activities the signal output intensifies significantly in the bandpass + moving average output graph. This indicates that it is possible to sense this activity with CSI-based sensing on the ESP32 when the correct filtering algorithm is chosen.

The large spikes at the beginning of the recording are likely caused by initializing the experiment. During this short period people were standing close to the laptop, and were therefore also close to the ESP32 configured as access point. The same phenomenon also appears at the end of the measurements. This is likely due to the same issue, namely people standing close to the laptop while ending the recording.

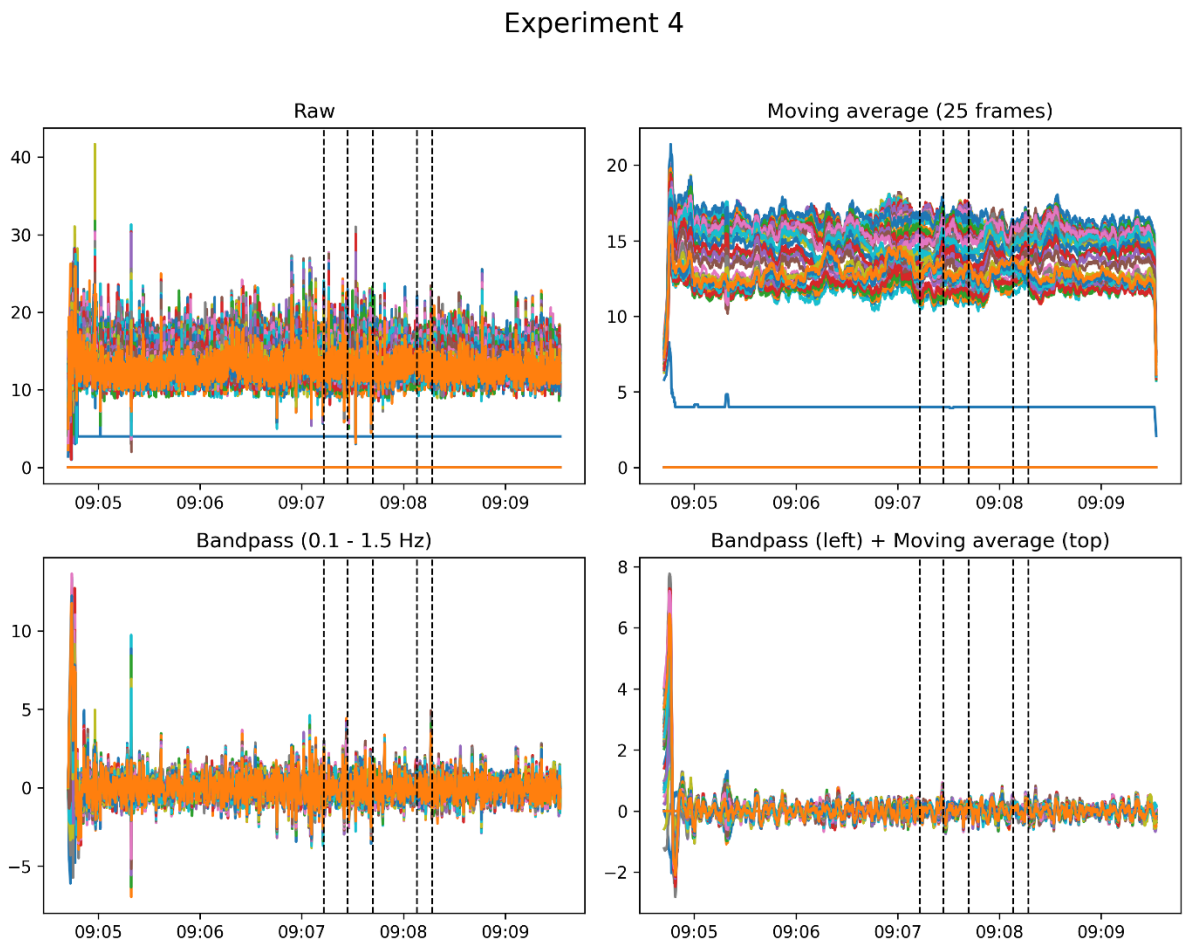

Figure 8: graphical output of experiment 4

In Figure 8 the results of a test participant walking through the LoS can be seen. In the graph created with a bandpass filter (0.1-1.5Hz) small peaks can be seen at the timestamps marked with black dotted lines. The bandpass + moving average filter does not show a lot of deviation from the standard noise signal. Therefore, it is not possible to claim that in this particular setup, the ESP32 would be able to detect a pedestrian walking through its LoS with another node 8 meters away.

A possible explanation why this setup was able to detect a bicycle and not a walking person might be due to the large metal frame of the bicycle. Metals are known to cause a lot of reflection artefacts with Wi-Fi signals, increasing the amount of useful incoming CSI data. Since this is not the case for a person walking, the current setup might not have antennas which are powerful enough to create a strong LoS line which can be used for detecting walking individuals.

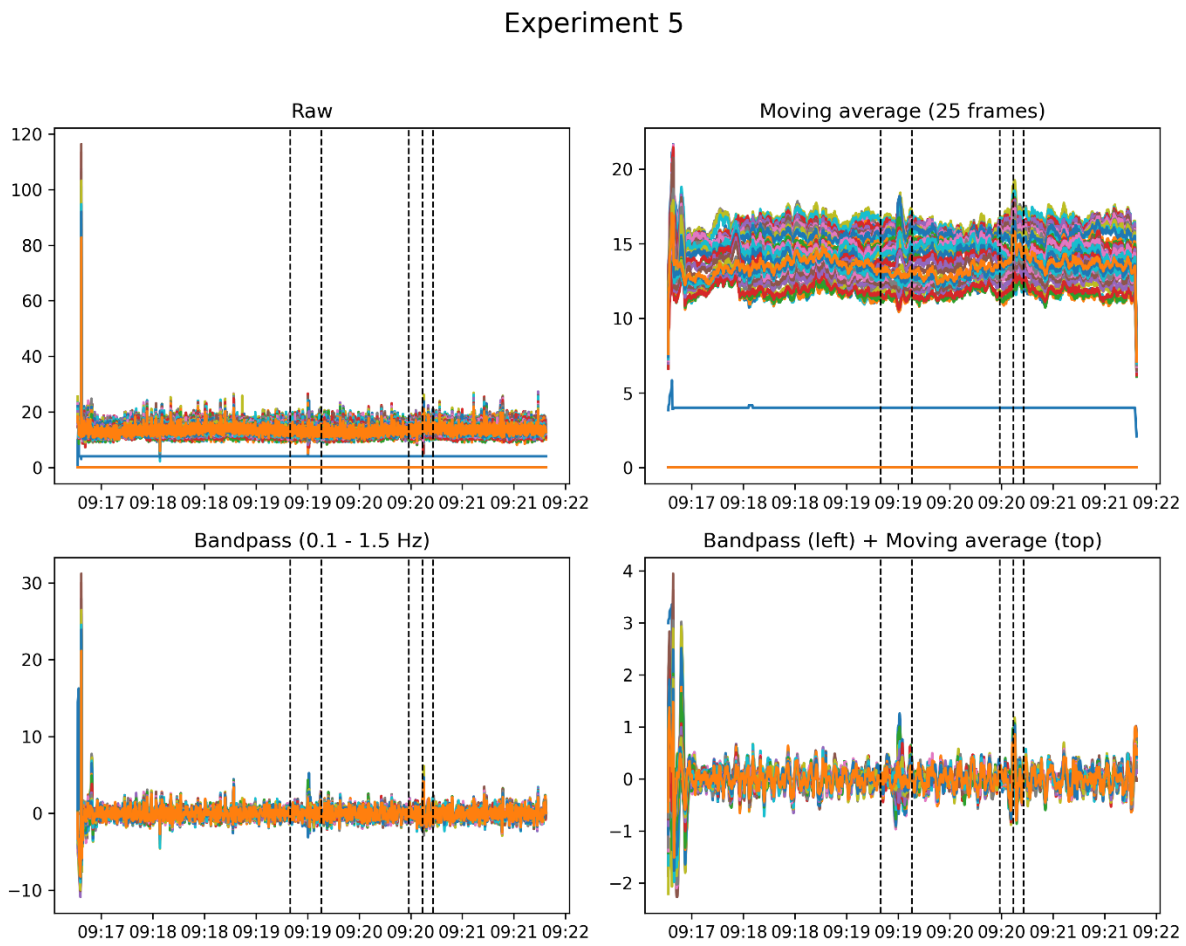

Figure 9: graphical output of experiment 5

For experiment 5, the results shown in Figure 9 show a clear difference in output signal passing through the bandpass + moving average filter compared to the noise in the idle state. In between the dotted timestamp bounds, a higher than usual signal difference can be seen. This is indication that the system would be able to detect this event if the right filtering algorithm was chosen.

In experiment 5, just like in experiment 3, it was possible again to detect the event happening. A similarity between experiment 3 and 5 is that in both experiments bicycles were involved. This makes the hypothesis (mentioned on the previous page) that the metal frame of the bicycles has something to do with the output results more feasible.

The evidence collected by the few experiments in this research is not strong enough to eighter confirm or deny this hypothesis, but this could be an interesting future experiment with the experiment setup in mind.

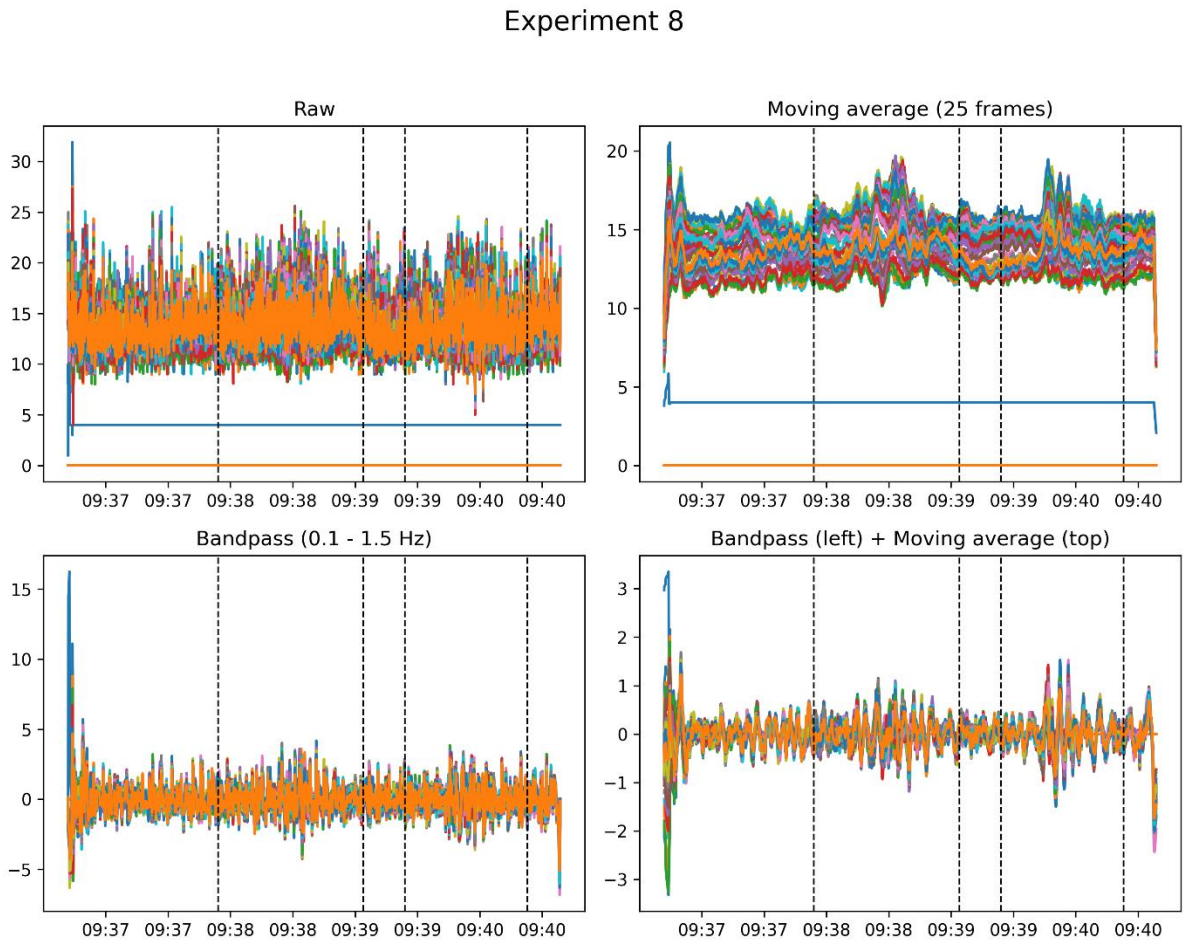

Figure 10: graphical output of experiment 8

The last experiment that will be highlighted in this results section is experiment 8. In this particular experiment, a test subject was instructed to walk towards the LoS, execute several poses in between the station and access point ESP32s, and continue walking to the end of the road. At the end of the road, the test subject turned around and walked back to the LoS. In the LoS, the test subject rotated a full 360° on their place before walking back to the start of the road. These timestamps are marked in Figure 10 as dotted lines. The first two lines are to indicate the start and ending of the poses, and the third and fourth line are for the start and the end of the rotation, respectively.

A significant change in the output signal through the bandpass + moving average filter can be seen. These changes occur exactly in between the bounds set by the timestamp lines. Because of this significant change in output, it can be assumed that the ESP32 is capable of detecting these events when the correct filtering algorithm is applied.

The end result of this series of experiments can be summarized as follows: The ESP32 microcontroller is capable of collecting useful CSI data for research and development applications. The particular ESP32 modules used in this experiment were generic-purpose modules with no optimalization for CSI applications. Even though some experiments did not deliver satisfactory results, mostly on the experiments containing walking related events, there is still a possibility that these results will improve once a purpose-built ESP32-based CSI data collection hardware tool is designed and optimized. The ESP32 is a solid starting point for CSI data collection applications, but might needs some fine-tuning or other additional components to achieve the best results for CSI applications.

The experiments that have been conducted for the sake of verification of the assumptions being made about the theoretical design during the design phase have been carefully constructed and set-up to mimic a real-world scenario as closely as possible. The experiments were initially designed to be executed on the real hardware once it was produced according to the specifications to do real-world testing on the physical product, but unfortunately it was not possible to produce the hardware within the time constraints of this project. Unforeseeable problems from the financial side caused delays within the production process which could not be resolved in time for the boards to be ready for the experiments.

All the experiments have been conducted on comparable hardware instead. This means that the results are not a perfect representation of the results that would have been collected with the real hardware. Although it is not a perfect representation, the results should still be fairly close to what would have been recorded with the real hardware, given the similarities within the test hardware. The microcontroller and the firmware are identical for both scenarios. One significant difference is the antenna configuration. Since the real device would use multiple real purpose-built antennas with better characteristics and the setup used for the experiment uses a simple integrated PCB antenna, it is only reasonable to assume that the results with the better antenna setup would give even better CSI return feedback. If a CSI event could be detected with the simple PCB antenna (which happened as can be seen in the results), it is fair to assume that the custom hardware board would return results that are at least as clear and significant. This makes the results collected with the alternative hardware (which was not the initial idea) valid for verifying the usefulness of the ESP32 microcontroller for CSI-based event detection.

Discussion and future work

The literature research, requirements analysis interviews, the experiments, and the hardware design process shed more light on the general concept of CSI analysis and the potential of this technology. Useful insights into the potential and challenges were discovered during the writing of this report. The primary goal of this project was to develop a robust and flexible hardware platform that can be used by developers and researchers interested in CSI analysis in an easy and efficient way.

At the start of this project it was the goal to design a proper useful hardware solution, and to place an order at an PCB assembly company to produce several prototype boards to evaluate the design decisions in a real-world application. Due to an unforeseen event in the financial department of the EEMCS-PS (University of Twente) committee, funding for this project could not be realized on time for the boards to be ready before the deadline of this report.

Due to the lack of a physical end product and a practical performance study with a prototype board, it is too early to say if the designed board is really suitable for the intended target application. There is also no feedback provided by test users yet, since the board could not be given out to researchers and developers for a functionality and practicality review.

Future work needs to be done in order to confirm and verify the results of this report. The boards should be ordered from a PCB and assembly services provider, and experiments should be conducted on said boards to verify their functionality and usability. These experiments should be run by the people in the target group of this product, researchers, and developers in the field of CSI-analysis. The feedback provided by the target group is always the most useful feedback for improving the design for a next revision.

Examples of the experiments that could be conducted are experiments to test the maximum range in which CSI packets can still be received, test the use of directional antennas with smart algorithms, battery life experiments using the sleep modes of the ESP32, and measuring the solar panel energy delivery in several weather conditions. If the participants of these experiments have any additional feedback, it should also be noted down and looked into during the designing of a next revision.

Conclusion

The ESP32 has proven itself as a suitable option for the microcontroller applied in CSI sensing. It is a flexible hardware platform with several useful features, and it has a very active developer base with a lot of example code and projects already available for testing. The experiments that were conducted sometimes showed signs of success, the ESP32 was able to collect CSI data which made recognizing certain activities possible.

Energy consumption of a demo board could greatly be reduced by initiating sleeping modes on the ESP32. The total consumption could be limited to such a low level that power harvesting becomes a feasible option for charging a battery to prepare for the event of a peak in energy consumption of the ESP32 when it wakes up from sleeping.

Designing a PCB for high-frequency (RF) applications is fairly different compared to a simpler design with a couple of DC components only. During the research of how to design PCBs for those kinds of applications, many useful insights were gathered related to PCB design.

Even though there is no physical product delivered at the time of this writing, this report still remains to form a solid beginning in the process of developing specialized CSI analysis hardware that could be used by developers and researchers in many different fields interested in the potential of CSI technology. Many important insights were given into the world of CSI analysis and hardware design for such applications. Future research can build further upon this report and its insights.

The research questions that were selected for the literature research chapter can be further answered and elaborated upon with the results provided by the practical experiments.

For the first question (‘For which type of applications are CSI-based systems usable?’), it has been proven that CSI data can be used to detect events happening in the LoS between the station and the access point. Events like walking and cycling through this LoS could be seen in the output results given the recorded timestamps of the events happening. This makes CSI-based sensing capable of at least recognizing the activities of walking and cycling through a LoS that has been set up beforehand.

Even though it is difficult to determine the exact level of accuracy achievable by CSI-based systems, the second question (‘What level of accuracy can be achieved with CSI-based systems?’) can still be partially answered given the results provided by the experiments. It was clear from the results that events could be detected, as the output data spiked at the given timestamps when the event happened. A simple algorithm could just look for spikes in the output data, and if a certain threshold value is reached and lowered to a normal value shortly after, an event could be detected. When the data would be analyzed in a more complex and thoughtful way, it is reasonable to assume that events could be triggered with higher accuracy without the problem of false positive detections. It is possible that a better setup (for which the specialized hardware designed in this project would be used) with real purpose-build antennas instead of integrated PCB antennas would increase the accuracy more by creating higher data spikes making it easier to detect events.

The desired environmental conditions that were previously mentioned in the literature research to answer the third question (‘What are desired environmental condictiones for CSI-technology?’). One of the results of this literature research mentioned that the distance between the access point and the station is very significant for the accuracy of the measurements. It was said that 2 meters is about as far as the nodes can be apart from each other without compromising accuracy. In the experiments the distance between the two nodes was set to be 8 meters. The experiment also took place in an outdoor environment instead of indoors, which is better for accuracy because of the walls bouncing back some of the waves making the data more detailed. Because the experiment was designed to show the benefits of the customized hardware in outdoor environments, the experiment conditions were not optimal for CSI data collection. Even though the environmental conditions were far from optimal, the

experiments returned useful and significant results. This proves that it is possible to collect useful CSI data even when the optimal conditions are not met. Using customized hardware to adapt to these sub-optimal conditions is a logical next step to increase accuracy.

As the literature research indicated for question four (‘Which type of MCUs/sensors are typically used in other research involving CSI-technology?’), many other research projects use different hardware than the ESP32 microcontroller series. In the experiments it has been proven several times that the ESP32 is just as capable for CSI research as other alternatives used by most other research. The open source software available made the ESP32 an easy hardware platform to develop for and to research the possibilities and limitations of CSI data.

The main research question of the background research (‘Is CSI-based position estimation and object recognition a feasible replacement for other technologies like radar?’) can partially be answered with the results from the practical experiments conducted. In this report it has been proven that CSI-based sensing is a good way to do activity recognition and human presence detection, which fall under the same category as position estimation. All those activities involve sensing humans. Object recognition has not been explicitly tested, but the cycling experiment did involve an object. As can be seen in the results, the output graphs of walking through the LoS and cycling through the LoS are significantly different. This suggests that it is possible to detect objects using CSI technology. More research needs to be conducted to prove the effectiveness for CSI analysis on object recognition, but in this report, it has been proven that CSI is a suitable replacement technology for sensing human activity and their position.

Appendices

Appendix 1


EASTPAK

Appendix 2

Consent Form for 'Designing a Wi-Fi CSI board for outdoor applications'

YOU WILL BE GIVEN A COPY OF THIS INFORMED CONSENT FORM

Please tick the appropriate boxes	Yes	No
Taking part in the study		
I have read and understood the study information dated 25/06/2024, or it has been read to me. I have been able to ask questions about the study and my questions have been answered to my satisfaction.	○	○
I consent voluntarily to be a participant in this study and understand that I can refuse to answer questions and I can withdraw from the study at any time, without having to give a reason.	○	○
I understand that taking part in the study involves walking and cycling through an area set up to record CSI data (as mentioned in the information sheet). I agree to engage in physical activities in the form of cycling and walking/running through the detection field. I understand that I am not forced to engage in any of these activities, and that I am able to withdraw for whatever reason or no reason at all if I choose to do so. I consent to this anonymous information to be stored, processed/analysed, and used in the final report of this research. I understand that none of the data recorded forms any risk for my own security/privacy, and is completely anonymous.	○	○
Use of the information in the study		
I understand that information I provide will be used for validating the effectiveness of the hardware used in the experiment for CSI environmental awareness applications. I understand that the information generated by this experiment will only be used in the final report of this research and in the presentation of the project. I understand that the data output of this experiment is not exposing my identity and is completely anonymous.	○	○
Future use and reuse of the information by others		
I give permission for the collected (anonymous) CSI raw data output that I provide by participating in this experiment to be stored in the additional/appendix section of the research report so it can be used for future research and learning. I understand that this data includes CSI frames which are not attached to any personal information and graphical output generated with this data. I understand that this data is for research purposes only and will not be forwarded to third parties or sold for commercial gain.	○	○
I agree that my information may be shared with other researchers for future research studies that may be similar to this study. The information shared with other researchers will not include any information that can directly identify me. Researchers will not contact me for additional permission to use this information.	○	○

UNIVERSITY OF TWENTE.

Signatures

Name of participant	Signature	Date
Hugo van 't Riet		
Researcher name	Signature	Date

Study contact details for further information:

Name: Hugo van 't Riet

Study: Bachelor Creative Technology

E-mail: h.vantriet@student.utwente.nl

Contact Information for Questions about Your Rights as a Research Participant

If you have questions about your rights as a research participant, or wish to obtain information, ask questions, or discuss any concerns about this study with someone other than the researcher(s), please contact the Secretary of the Ethics Committee/domain Humanities & Social Sciences of the Faculty of Behavioural, Management and Social Sciences at the University of Twente by ethicscommittee-hss@utwente.nl

UNIVERSITY OF TWENTE.

Appendix 3

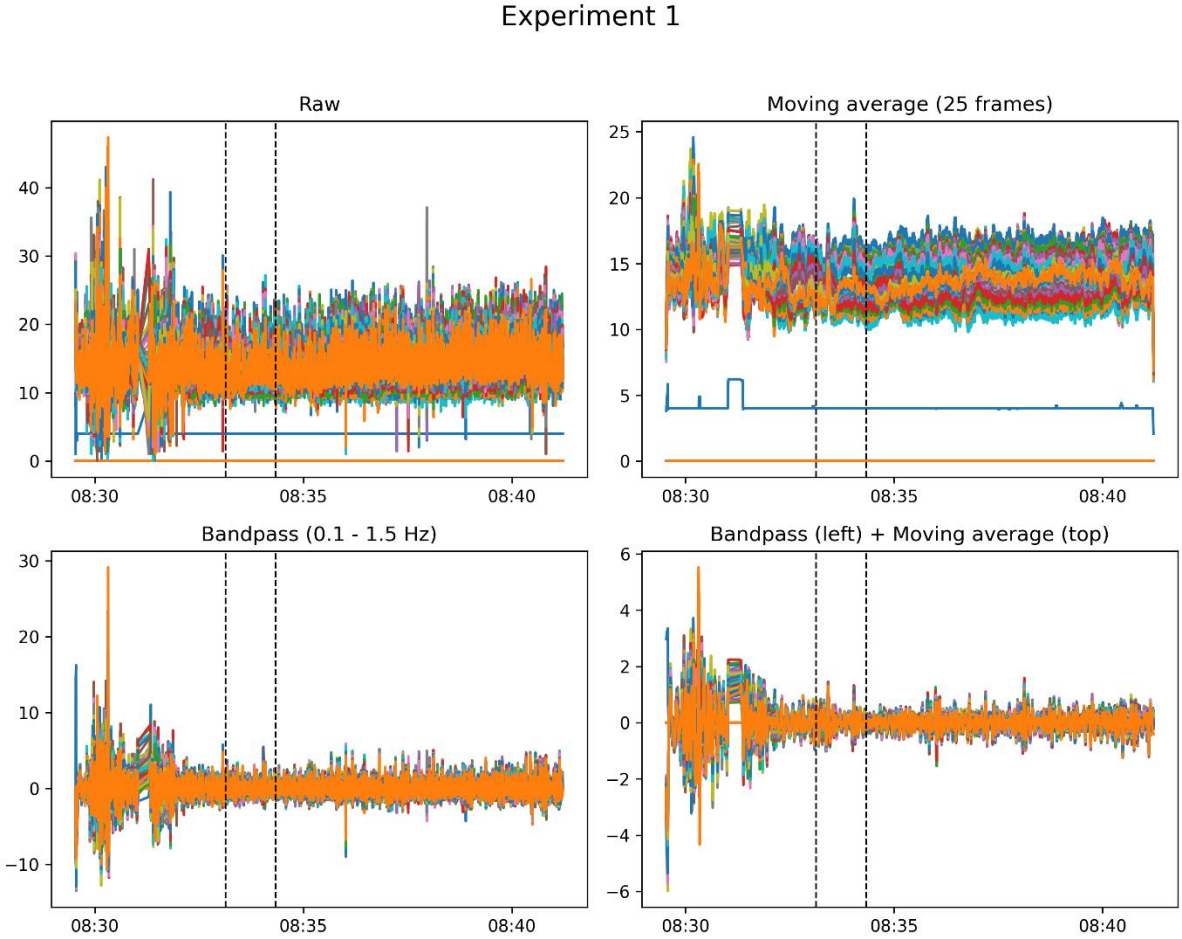
Experiment 1
Raw
Moving average (25 frames)
Bandpass (0.1 - 1.5 Hz)
Bandpass (left) + Moving average (top)
08:30
08:35
08:40

Experiment 2

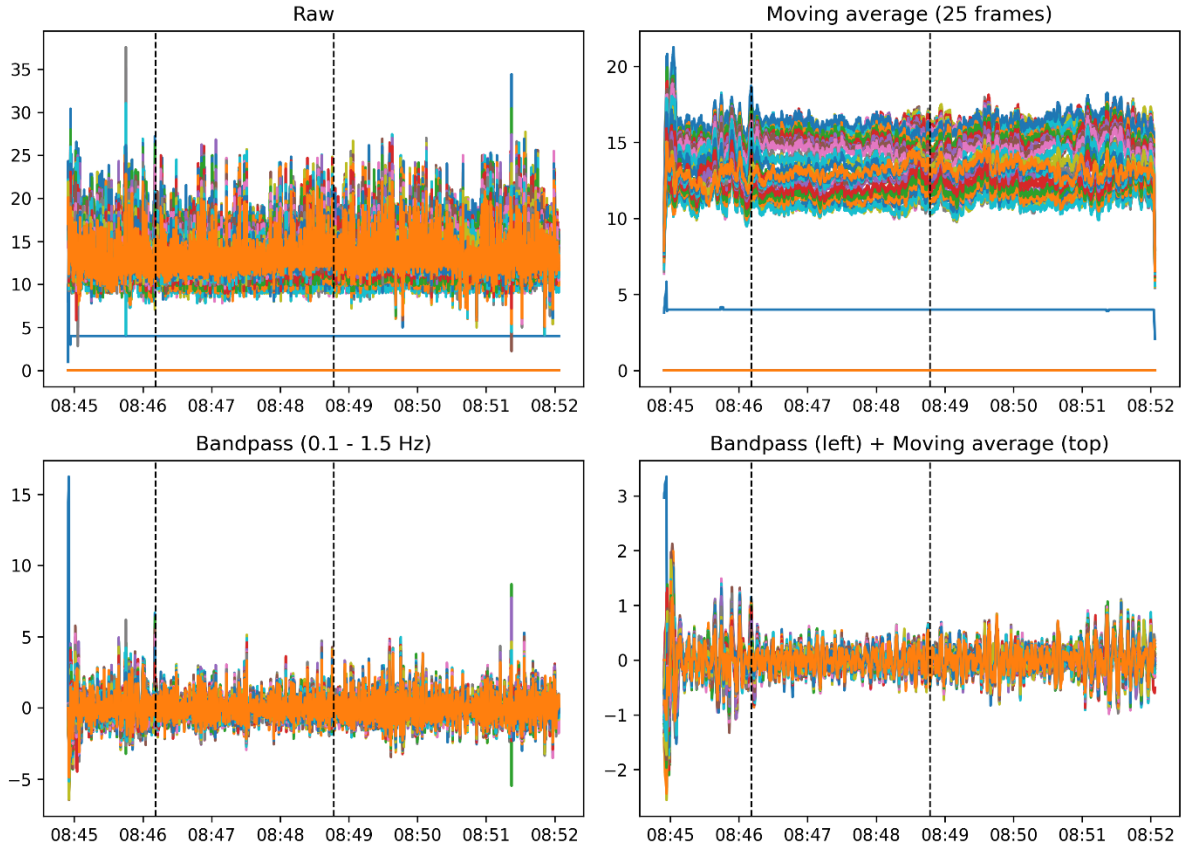

Experiment 3

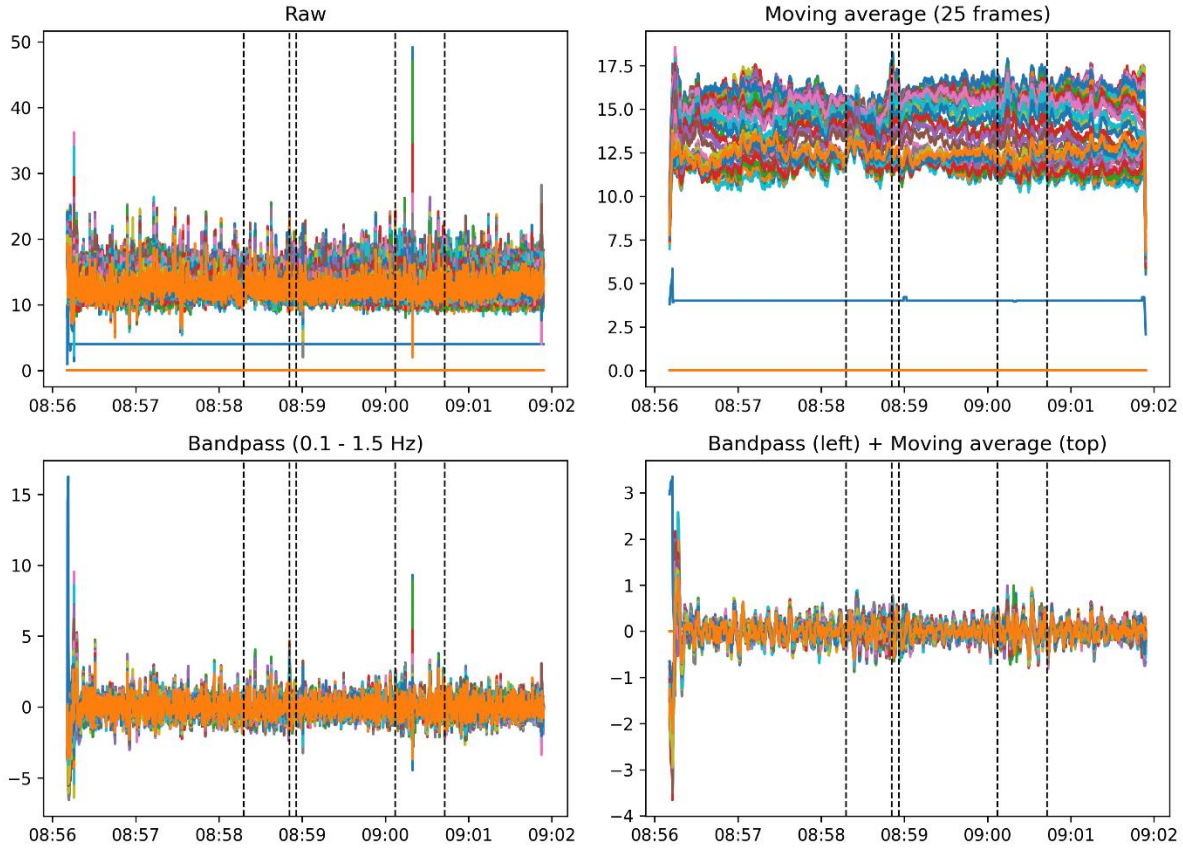

Experiment 4

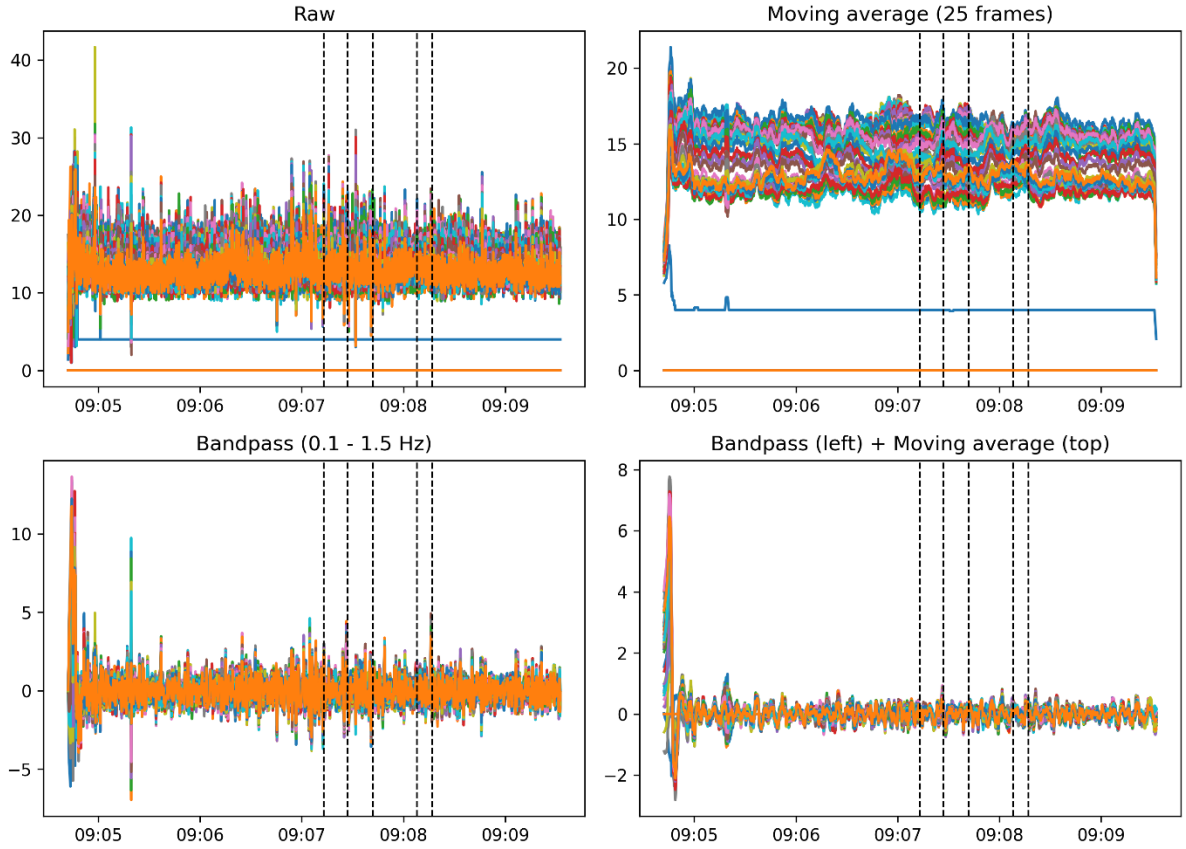

Experiment 5

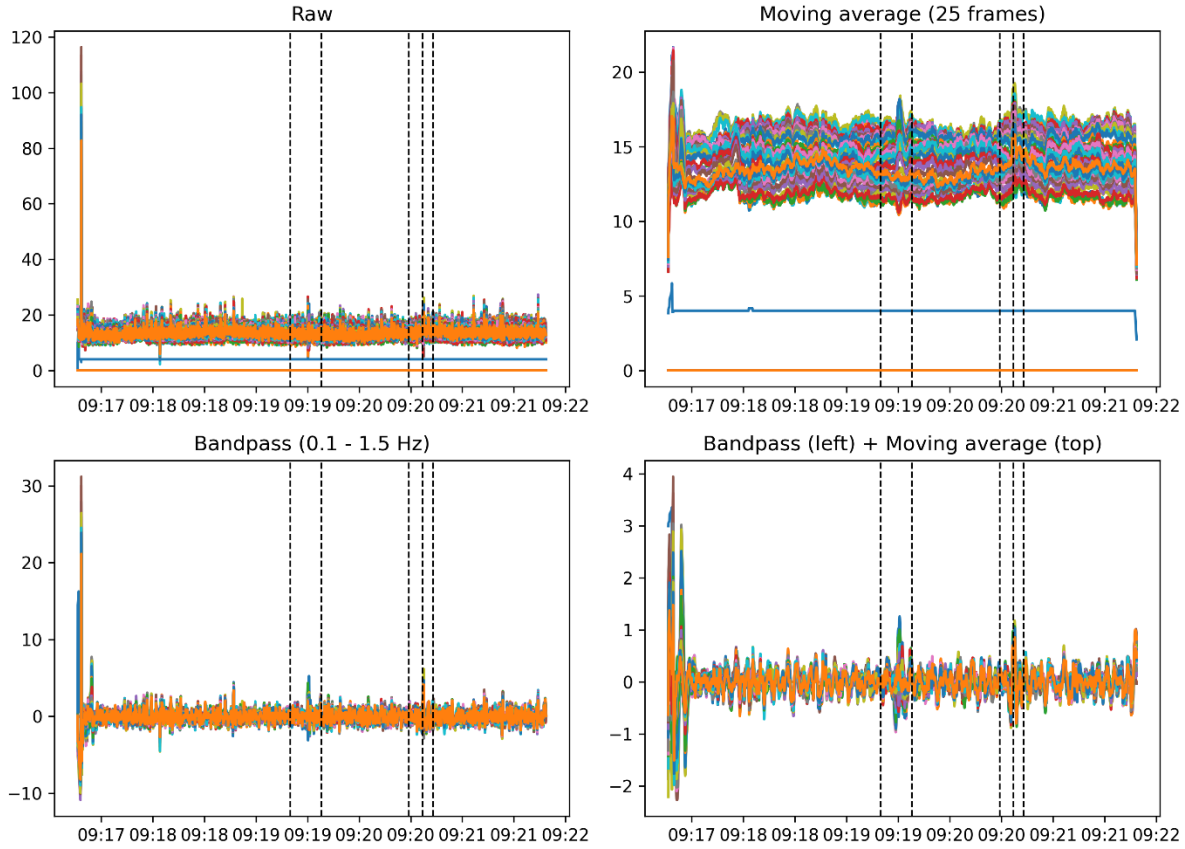

Experiment 6

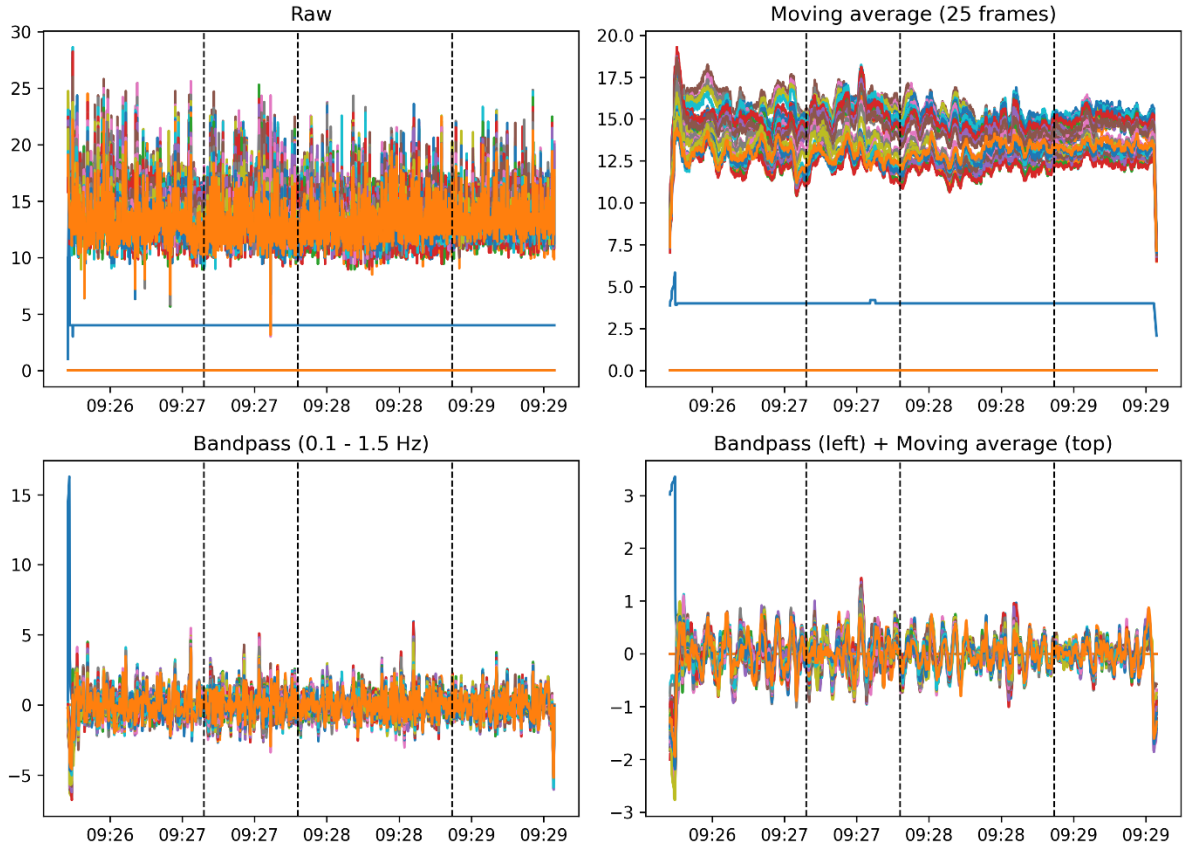

Experiment 7

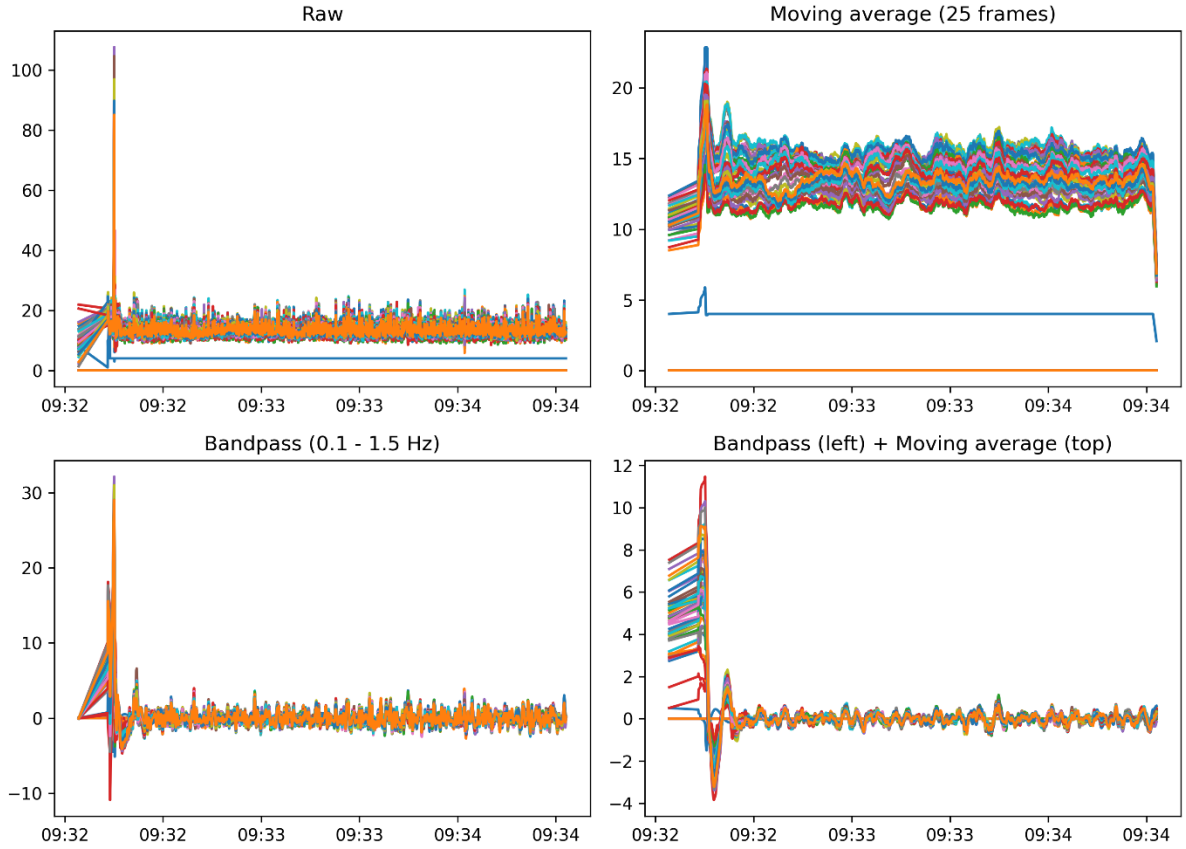

Experiment 8

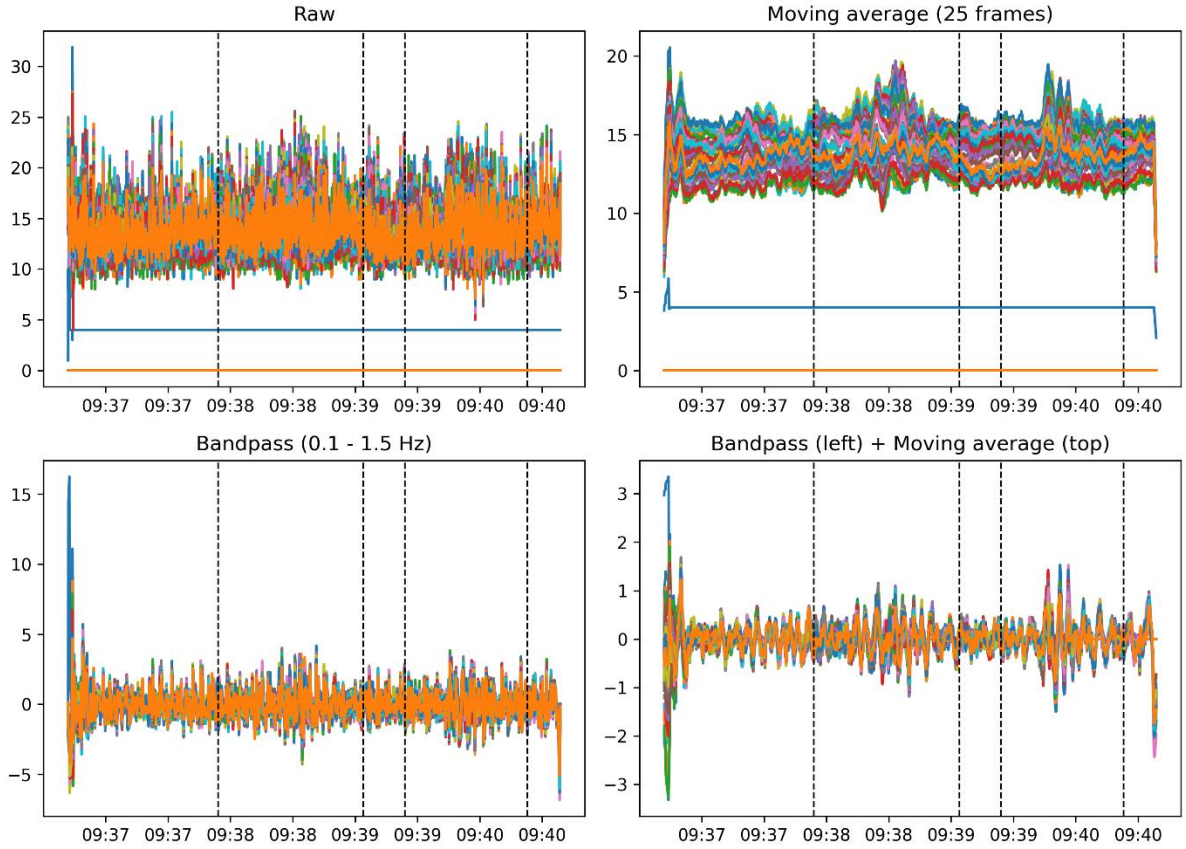

References

[1] L. S. Vailshery, “IOT connected devices worldwide 2019-2030,” Statista, https://www.statista.com/statistics/1183457/iot-connected-devices-worldwide/ (accessed Feb. 22, 2024).

[2], X. Lu, P. Zhao, and J. Chen, “Device-free presence detection and localization with SVM and CSI fingerprinting,” *IEEE Sensors Journal*, vol. 17, no. 23, pp. 7990–7999, Dec. 2017. doi:10.1109/jsen.2017.2762428

[3] O. Oshiga *et al.*, “Human detection for crowd count estimation using CSI of WIFI Signals,” *2019 15th International Conference on Electronics, Computer and Computation (ICECCO)*, Dec. 2019. doi:10.1109/icecco48375.2019.9043195

[4] T. Hang *et al.*, “Wish: WIFI-based real-time human detection,” *Tsinghua Science and Technology*, vol. 24, no. 5, pp. 615–629, Oct. 2019. doi:10.26599/tst.2018.9010091

[5] K. Qian *et al.*, “Enabling contactless detection of moving humans with dynamic speeds using CSI,” *ACM Transactions on Embedded Computing Systems*, vol. 17, no. 2, pp. 1–18, Jan. 2018. doi:10.1145/3157677

[6] T. Murakami, M. Miyazaki, S. Ishida, and A. Fukuda, “Wireless LAN-based CSI Monitoring System for object detection,” Electronics, vol. 7, no. 11, p. 290, Nov. 2018. doi:10.3390/electronics7110290

[7] M. Peng, B. Ge, X. Fu, and C. Kai, “Wi-tar: Object detection system based on CSI ratio,” IEEE Sensors Journal, pp. 1–1, Apr. 2024. doi:10.1109/jsen.2024.3384703

[8] C. Wang, J. Liu, Y. Chen, H. Liu, and Y. Wang, “Towards in-baggage suspicious object detection using commodity WIFI,” *2018 IEEE Conference on Communications and Network Security (CNS)*, May 2018. doi:10.1109/cns.2018.8433142

[9] S. Palipana, P. Agrawal, and D. Pesch, “Channel state information based human presence detection using non-linear techniques,” *Proceedings of the 3rd ACM International Conference on Systems for Energy-Efficient Built Environments*, Nov. 2016. doi:10.1145/2993422.2993579

[10] C. Han, Q. Tan, L. Sun, H. Zhu, and J. Guo, “CSI frequency domain fingerprint-based passive indoor human detection,” *Information*, vol. 9, no. 4, p. 95, Apr. 2018. doi:10.3390/info9040095

[11] C. M. Mesa-Cantillo *et al.*, “A non intrusive human presence detection methodology based on channel state information of Wi-Fi Networks,” *Sensors*, vol. 23, no. 1, p. 500, Jan. 2023. doi:10.3390/s23010500

[12] D. Halperin, W. Hu, A. Sheth, and D. Wetherall, “Linux 802.11n CSI Tool,” Linux 802.11n CSI tool, https://dhalperi.github.io/linux-80211n-csitool/ (accessed Apr. 10, 2024).

[13] F. Wang, S. Zhou, S. Panev, J. Han, and D. Huang, “Person-in-WIFI: Fine-grained person perception using WIFI,” 2019 IEEE/CVF International Conference on Computer Vision (ICCV), Oct. 2019. doi:10.1109/iccv.2019.00555

[14] S. M. Hernandez, “ESP32 CSI Toolkit,” ESP32 CSI toolkit, https://stevenmhernandez.github.io/ESP32-CSI-Tool/ (accessed Jun. 23, 2024).

[15] S. Bowden and C. Honsberg, “IV curve,” PVEducation, https://www.pveducation.org/pvcdrom/solar-cell-operation/iv-curve (accessed Jul. 2, 2024).

[16] “Designing high-frequency PCBS,” Sierra Circuits, https://www.protoexpress.com/kb/designing-high-frequency-pcbs/ (accessed Jul. 5, 2024).